

Copyright
by
Michael Lee Brack
1996

**THE EFFECT OF OPENINGS ON A PRECAST INFILL WALL
SEISMIC STRENGTHENING SYSTEM**

by

Michael Lee Brack, B.S., B.A.

Thesis

Presented to the Faculty of The Graduate School
of The University of Texas at Austin
in Partial Fulfillment
of the Requirements
for the Degree of

Master of Science in Engineering

The University of Texas at Austin

August 1996

**THE EFFECT OF OPENINGS ON A PRECAST INFILL WALL
SEISMIC STRENGTHENING SYSTEM**

APPROVED BY

SUPERVISING COMMITTEE:

James O. Jirsa, Supervisor

Michael E. Kreger

For Erin

ACKNOWLEDGMENTS

I would like to thank Dr. James O. Jirsa, thesis supervisor, for his guidance and encouragement. In addition to his technical expertise, his personal, professional, and travel advice have proven to be invaluable. I also thank Dr. Michael E. Kreger for his contributions to this project and for advising me throughout my career at The University.

To my wife, Erin, and our families for loving and supporting me during this endeavor: you have made so much of this possible.

To Robert Frosch, a true friend, I owe you an enormous debt of gratitude for pouring your heart into this project and for being my mentor along the way. Also, thank you to Wanzhi Li for his work in the phases of the project preceding this research.

I would like to express my gratitude to each of the people at the Phil M. Ferguson Laboratory for their help along the way: to my fellow students who volunteered their time to help with the “dirty” work, and to Blake Stassney and the rest of the Staff for providing their support in each phase of this project.

A sincere thank you goes out to the sponsor of this project, the National Science Foundation, for making this program possible. Thanks also to Loring Wyllie, Jr. of Degenkolb Engineers and Tom Sabol of Englekirk and Sabol Consulting Engineers.

In all things, to God be the Glory, for great things He has done.

Michael L. Brack

May 27, 1996

THE EFFECT OF OPENINGS ON A PRECAST INFILL WALL
SEISMIC STRENGTHENING SYSTEM

by

Michael Lee Brack, M.S.E.
The University of Texas at Austin, 1996
Supervisor: James O. Jirsa

Many existing structures are in need of seismic rehabilitation to avoid undergoing catastrophic collapse during a severe seismic event. A new, potentially economical method of strengthening has been developed which uses precast concrete panels to create an infill wall in a concrete frame building. A large-scale model using this method has been tested with positive results at the University of Texas' Phil M. Ferguson Structural Engineering Laboratory. The subject of this report is an investigation into the effect of architecturally required openings on the precast infill system.

To examine the effects of such openings on the precast panel infill system, selected panels were removed from the original model to create first a window, and then a doorway in the wall. Tests were performed on the structure in each configuration in the same manner as the previous research.

The performance of the system in each of these configurations is evaluated, and the results are compared with behavior of the full infill. The experimental results are also compared with calculations of the wall's strength and stiffness using conventional methods, including ACI design procedures. Finally, commentary is provided on the performance of the system with openings, and areas of caution and potential improvement are suggested.

TABLE OF CONTENTS

LIST OF TABLES	xi
LIST OF FIGURES	xii
CHAPTER 1: INTRODUCTION	1
1.1 Introduction.....	1
1.2 Background.....	1
1.2.1 Repair and Strengthening of Structures.....	1
1.2.2 Nonductile Frames.....	2
1.2.3 Infill Walls.....	4
CHAPTER 2: EXPERIMENTAL PROGRAM	6
2.1 Introduction.....	6
2.2 Existing Frame.....	7
2.2.1 Prototype Frame.....	7
2.2.2 Design and Details.....	7
2.2.3 Construction.....	11
2.3 Connection Tests.....	14
2.3.1 Panel Connection Tests.....	15
2.3.1.1 Test Variables.....	17
2.3.1.2 Results.....	18
2.3.2 Frame Connection Tests.....	20
2.3.2.1 Test Variables.....	22
2.3.2.2 Results.....	22

2.4 Infill Wall.....	23
2.4.1 Infill Wall Construction.....	25
2.5 Removal of Infill Panels	31
2.6 Material Data	34
2.6.1 Concrete	34
2.6.2 Steel Reinforcing Bars.....	36
2.6.3 Steel Pipes.....	36
2.6.4 External Post-Tensioning Steel.....	37
2.7 Test Setup	38
2.7.1 Loading System	38
2.7.2 Data Acquisition	41
CHAPTER 3: SPECIMEN HISTORY AND PRE-TEST CONDITION	42
3.1 Introduction.....	42
3.2 Bare Existing Frame Test	42
3.2.1 Performance	43
3.2.2 Damage	43
3.3 Full Infill Flexure Test.....	44
3.3.1 Performance	45
3.3.2 Damage	45
3.4 Full Infill Shear Tests	49
3.4.1 Performance	50
3.4.2 Damage	52
3.5 Damage and Repairs to the Loading System.....	52
3.6 Condition of the Specimen	56
CHAPTER 4: EXPERIMENTAL RESULTS.....	58

4.1 Introduction.....	58
4.2 Window Test.....	58
4.2.1 Preliminary Observations on Panel Removal.....	58
4.2.2 Structural Behavior.....	60
4.2.2.1 West Direction.....	60
4.2.2.2 East Direction.....	62
4.3 Door Test.....	64
4.3.1 Preliminary Observations on Panel Removal.....	64
4.3.2 Structural Behavior.....	66
4.3.2.1 West Direction.....	66
4.3.2.2 East Direction.....	70
CHAPTER 5: ANALYSIS	71
5.1 Introduction.....	71
5.2 Strength.....	71
5.2.1 Strength With and Without Openings.....	71
5.2.2 Strength Prediction of Infill with Window.....	72
5.2.3 Strength Prediction of Infill with Door.....	75
5.3 Stiffness.....	80
5.3.1 Introduction.....	80
5.3.2 Methodology.....	81
5.3.3 Stiffness Comparisons.....	84
5.3.3.1 Window Test.....	84
5.3.3.2 Door Test.....	85
5.4 Design and Construction Needs of Infills with Openings.....	89
CHAPTER 6: SUMMARY AND CONCLUSIONS	91

6.1 Summary	91
6.2 Conclusions and Recommendations	92
BIBLIOGRAPHY	94
VITA	95

LIST OF TABLES

Table 2. 1: Concrete Mix Data	35
Table 2. 2: Concrete Compressive Strengths.....	35
Table 2. 3: Reinforcing Steel Properties.....	36
Table 2. 4: Steel Pipe Properties.....	37
Table 2. 5: Individual Pipe Shear Capacities.....	37
Table 2. 6: Post-Tensioning Steel Strengths.....	38
Table 5. 1: Infill Strength with Openings	72
Table 5. 2: Summary of Calculated Strengths vs. Tested Strength for Infill with Window.....	75
Table 5. 3: Flexural Strength of Infill with Door.....	79
Table 5. 4: Stiffness Comparison: Window vs. Full Infill.....	85
Table 5. 5: Stiffness Comparison: Door vs. Full Infill	88

LIST OF FIGURES

Figure 1.1: Frame Failure Mechanisms	3
Figure 2. 1: Typical 1950's and '60's RC Frame	8
Figure 2. 2: Existing Frame of Test Structure	9
Figure 2. 3: Beam-Column Joint in Test Specimen.....	10
Figure 2. 4: Footing Construction.....	12
Figure 2. 5: First Story Construction	12
Figure 2. 6: Completed First Story	13
Figure 2. 7: Second Story Construction.....	13
Figure 2. 8: Completed Existing Frame.....	14
Figure 2. 9: Panel Connection Specimen.....	15
Figure 2. 10: Panel Connection Details	16
Figure 2. 11: Panel Connection Test Variables	18
Figure 2. 12: Typical Panel Connection Test Results.....	19
Figure 2. 13: Frame Connection Specimen	21
Figure 2. 14: Frame Connection Details.....	21
Figure 2. 15: Typical Frame Connection Test Results	23
Figure 2. 16: Infill Wall Installed in Original Frame.....	24
Figure 2. 17: Precast Panel Formwork and Reinforcing.....	25
Figure 2. 18: Infill Construction Sequence.....	27
Figure 2. 19: Crane Used for Panel Placement.....	28
Figure 2. 20: Panel Placement Using Inserts and Braces	28
Figure 2. 21: Rebar and Pipe Placement.....	29
Figure 2. 22: Closure Strips Formed for Casting Stage 2.....	30
Figure 2. 23: Panel Casting Operation During Casting Stage 4	31
Figure 2. 24: Panel Sawing Operation.....	32

Figure 2. 25: Wall with Window	33
Figure 2. 26: Wall with Doorway at Second Level	33
Figure 2. 27: Test Setup.....	39
Figure 2. 28: Displacement Gage Locations.....	40
Figure 2. 29: Strain Gage Locations	41
Figure 3. 1: Behavior of Full Infill Prior to Splice Failure During Flexure Test	46
Figure 3. 2: Behavior of Full Infill Wall During Flexure Test	46
Figure 3. 3: Cracking Pattern in the Full Infill Wall.....	48
Figure 3. 4: Main Compression Struts in Full Infill	48
Figure 3. 5: Behavior of Full Infill During First Shear Test.....	50
Figure 3. 6: Behavior of Specimen During Final Shear Test	51
Figure 3. 7: Failed Loading System at Third Floor, Viewed From the Southwest.....	53
Figure 3. 8: Connection of Bracing System to Column.....	55
Figure 3. 9: Brace for the Loading System.....	56
Figure 4. 1: Cracks in Window Panel Prior to Removal	59
Figure 4. 2: Window Test: Loading History.....	61
Figure 4. 3: Window Test: Load vs. Drift Response	61
Figure 4. 4: Damage During Window Test.....	63
Figure 4. 5: Crushing at Toe of Wall.....	63
Figure 4. 6: Cracking at Failure of Window Configuration	64
Figure 4. 7: Door Configuration	65
Figure 4. 8: Door Test: Loading History	67
Figure 4. 9: Door Test: Load vs. Drift Response.....	67
Figure 4. 10: Failed Coupling Beam During West Direction Loading.....	68
Figure 4. 11: Buckled Reinforcement in Closure Strip	69
Figure 4. 12: Base Crack at Doorway.....	69
Figure 4. 13: Failed Coupling Beam During East Direction Loading.....	70

Figure 5. 1: Force Flow Around Window.....	73
Figure 5. 2: Compression Struts During Window Test	76
Figure 5. 3: Uncoupled and Fully Coupled Behavior.....	78
Figure 5. 4: Coupling Beam Region	80
Figure 5. 5: Secant Stiffness Determination (Window Test Shown).....	82
Figure 5. 6: Rigid Body Rotation Effects	84
Figure 5. 7: Three Methods of Determining Rigid Body Rotation Effects	87

CHAPTER 1

INTRODUCTION

1.1 Introduction

Reinforced concrete infill walls are a proven method of strengthening nonductile concrete frame structures for seismic events. Previous studies^[7, 9, 10] at The University of Texas at Austin have shown that weak links in frame systems can be overcome by installing a cast-in-place concrete infill wall in the frame. These walls are typically connected to the existing frame with steel dowels, and have continuous steel over their height to overcome inadequate lap splices in the columns. In a study recently completed at The University of Texas at Austin, a new type of infill wall system was tested with favorable results.^[6] The new system utilized precast concrete panels which were grouted into place, along with unbonded external tensile reinforcement. The precast panel system minimizes the volume of concrete which must be cast in place and eliminates the numerous interface dowels required in current methods, which are expensive to install. The purpose of this study is to investigate the effect of openings on this new infill wall system for strengthening reinforced concrete frames in seismic zones.

1.2 Background

1.2.1 Repair and Strengthening of Structures

With each major earthquake, more knowledge is gained about the performance of structures under seismic loads. As understanding of the behavior of structures in earthquakes has increased, improvements have been made in the

way these structures are analyzed, designed, and constructed. It has also become clear that many existing buildings are in need of strengthening in order to meet current code standards and sound engineering principles. In addition, it is often more cost effective to repair damaged structures than to replace them. For these reasons, there is a need for economical and efficient techniques for strengthening seismically deficient structures. Many systems and methods of strengthening structures are currently used. The choice of an appropriate system for a given structure depends on the structural characteristics and details of that structure, as well as cost, owner/occupant requirements and architectural considerations. Among the most common methods of strengthening concrete structures are column jacketing, steel bracing, and the addition of infill walls to the structure.

1.2.2 Nonductile Frames

Nonductile frames are likely candidates for seismic strengthening. These structures, often low- to mid-rise office buildings, were commonly constructed in the 1950's and '60's in California, and were designed according to the provisions of the Uniform Building Code^[11], which incorporated the ACI 318-56^[11] and ACI 318-63^[2] codes. These codes specified design loads that are significantly lower than the forces generated during elastic response of structures to earthquake loads. Structures designed as such must have a reserve of ductile deformation capacity in order to withstand deformations imposed by severe earthquakes. Due to certain key weaknesses commonly found in the design and detailing of nonductile frames, however, these buildings often lack this necessary ductility.

Deficiencies in nonductile frames generally stem from inadequate shear or flexural capacity, and from details that cause brittle failures to occur before more ductile failure modes. Common problems with these structures include: lack of

confinement in potential hinging regions; inadequate shear or flexural reinforcement required to resist seismic load reversals; column lap splices that occur in regions of high moments (e.g., just above the floor levels) and are not long enough to develop tensile yield of the longitudinal bars; lack of confinement in beam-column joints; and inadequate joint shear capacity.

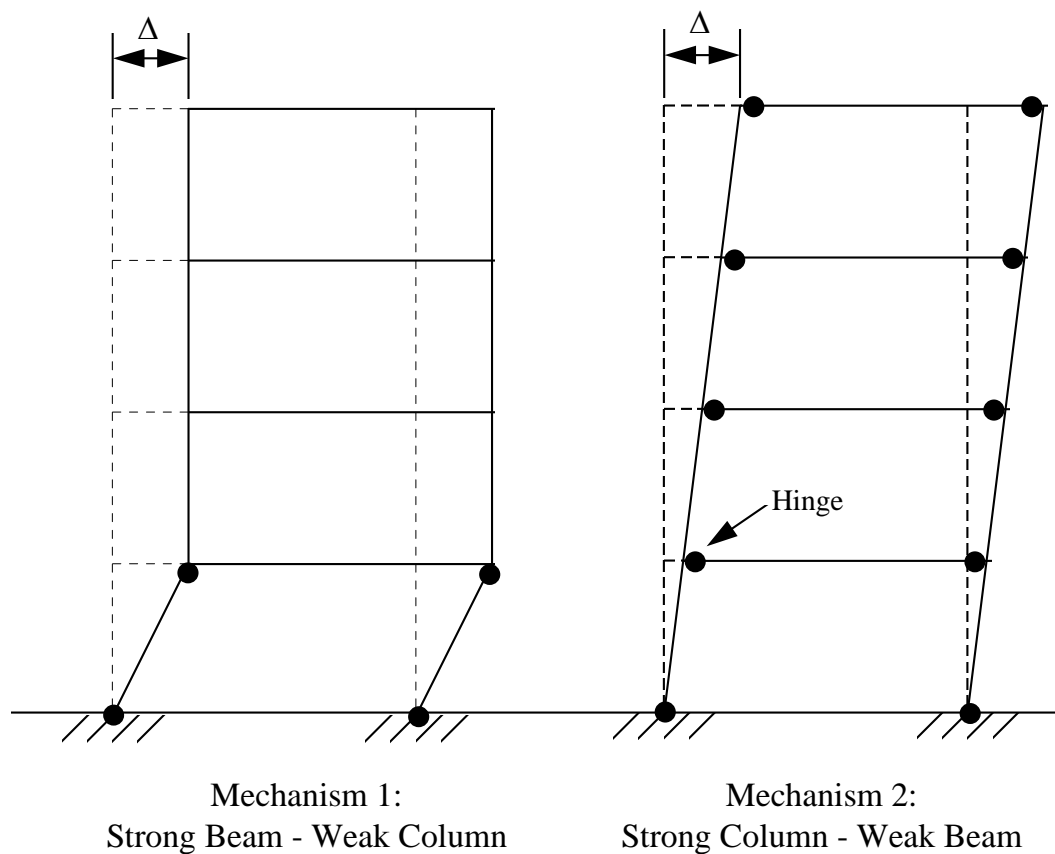


Figure 1.1: Frame Failure Mechanisms^[6]

Figure 1.1 illustrates two failure mechanisms for frame structures under lateral loads. Often in nonductile frames, the flexural capacity of the beams is greater than that of the columns, creating a strong beam-weak column system.

The failure mode for this type of system is a collapse mechanism (Mechanism 1) involving only the columns. Column hinging may be difficult to repair and may lead to lateral instability under gravity loads. A strong column-weak beam system has a more desirable failure mechanism (Mechanism 2) in which the beams yield, but overall stability of the structure under gravity loads is retained. This type of system is known as a strong column-weak beam system.

Because of the many problems associated with the members of nonductile frames, adding infill walls is often a favorable strengthening technique. The infill walls effectively bypass the weaknesses of the system by carrying the majority of the seismic loads themselves, diverting forces from the frame.

1.2.3 Infill Walls

Infill walls can greatly increase the strength and stiffness of a frame system. While walls tend to increase slightly the mass of the structure, and thus the inertia forces that must be resisted in an earthquake, this effect is offset by the large increase in lateral resistance provided by the walls. Properly designed, walls can develop ductile failure modes and bypass more brittle failure modes that might occur in an unstrengthened frame. The use of infill walls can create difficulties in the structure, however, including a limitation of architectural space and flexibility, and increased forces at a concentrated area of the foundation. Forces generated at the base of an infill wall during a seismic event can be greater than the capacity of the existing foundation. If modifications to the foundation are required to support the wall, this can greatly increase the cost of any strengthening scheme.

Traditionally, infill walls are cast in place or shotcreted into the existing frame. These methods require the installation of numerous steel dowels into the existing frame in order to achieve monolithic behavior of the wall with the frame.

The high costs associated with the placement of these dowels is one negative aspect of these systems. Other negative aspects associated with the construction of infill walls is the need for large amounts of fresh concrete to be placed (particularly troublesome if walls are to be placed in interior bays of the structure) and the need for extensive formwork.

The infill wall system that is the subject of this study, however, has the potential to overcome some of these undesirable characteristics. The majority of the space in the bay to be infilled is taken up by several precast reinforced concrete panels that can easily be moved into position, and concrete is cast into the remaining spaces. This reduces the amount of fresh concrete and formwork that must be brought into the building. Rather than using numerous dowels, connection to the original frame is made by fewer, larger steel pipes, saving time and construction cost. Tensile capacity is provided by external unbonded bars anchored at the foundation and the top of (or along) the wall, to overcome weaknesses associated with column splices.

CHAPTER 1	1
1.1 Introduction	1
1.2 Background	1
1.2.1 Repair and Strengthening of Structures	1
1.2.2 Nonductile Frames	2
1.2.3 Infill Walls	4
Figure 1.1: Frame Failure Mechanisms	3

CHAPTER 2

EXPERIMENTAL PROGRAM

2.1 Introduction

The experimental program that is the subject of this report is an extension of a previous program conducted at the Phil M. Ferguson Laboratory at the University of Texas at Austin. The previous experimental program investigated the performance of the precast reinforced concrete panel infill wall system as a full infill. The previous program consisted of three phases: (I) investigation of panel-to-panel connections; (II) investigation of panel-to-frame connections; and (III) construction and testing of a 2/3 scale model frame with a full infill wall installed. The tests in the current program (phase IV) utilized the scale model frame and infill wall from the previous program (phases I-III).

This chapter provides background information from phases I-III while describing the detailing and construction of the test specimen, and introduces the experimental program of phase IV. For a complete discussion of phases I-III of the program, see Reference 6. Section 2.2 describes the existing frame used as a basis for testing the infill strengthening system. In Section 2.3, the two types of connection tests (phases I and II) are outlined and key results are presented. Section 2.4 then develops the details and construction of the infill wall itself (phase III), which was installed in the existing frame and was based on the results of the connection tests. The removal of the infill panels in preparation for phase IV is discussed in Section 2.5. Sections 2.6 and 2.7 then describe the materials used in the tests and test setup. Chapter 3 is devoted to describing the loading history and condition of the model frame specimen at the start of the current tests (phase IV).

2.2 Existing Frame

2.2.1 Prototype Frame

The existing frame structure was modeled after a reinforced concrete moment resisting frame building typical of construction in the 1950's and '60's. Such a structure is presented in Figure 2.1. The gravity load system of this structure is a one-way slab supported by a system of girders and columns. A large number of these structures, commonly two- to five-stories tall, exist today.

2.2.2 Design and Details

Two stories of a typical interior frame from the prototype structure were taken as the basis for the model structure. The prototype frame design was scaled down by a factor of $2/3$. This scale was chosen to result in a model size compatible with testing facilities at the Ferguson Laboratory, while remaining a relatively large-scale model. The resulting specimen had 8 ft. story heights and a 13 ft. - 4 in. bay spacing. The specimen is depicted in Figure 2.2.

Two features were built into the existing frame to simulate beam-column joint conditions in an interior frame. First, the floor beams were extended beyond the columns. In addition to balancing beam moments imposed on the columns, these cantilevers allowed beam top reinforcement to be continued through the columns. Second, column stubs were constructed at the top floor to allow longitudinal column reinforcement to extend through the joint. As a result, no special anchorages of beam or column bars were required at the joints in the model.

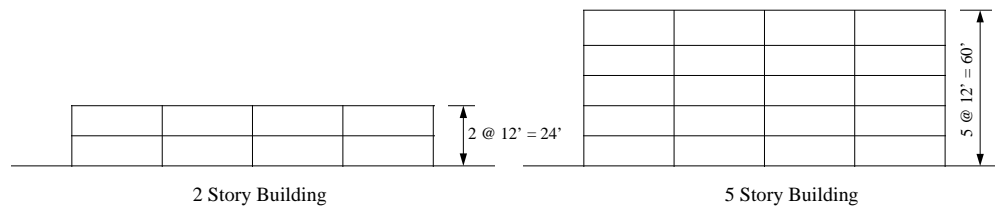
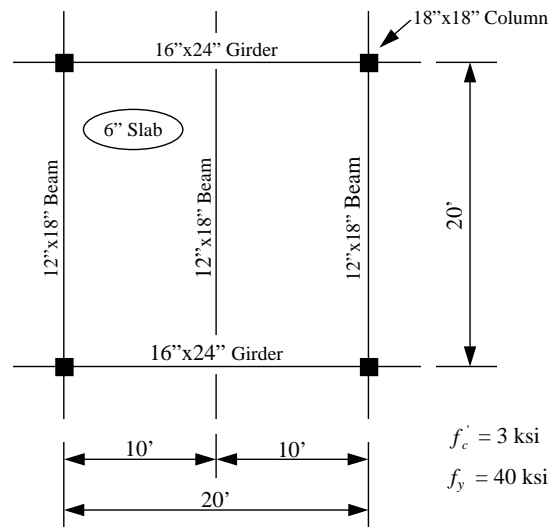


Figure 2.1: Typical 1950's and '60's RC Frame^[6]

The details of the model frame were designed to reflect the major nonductile features typical of construction in the 1950's and '60's. These features include:

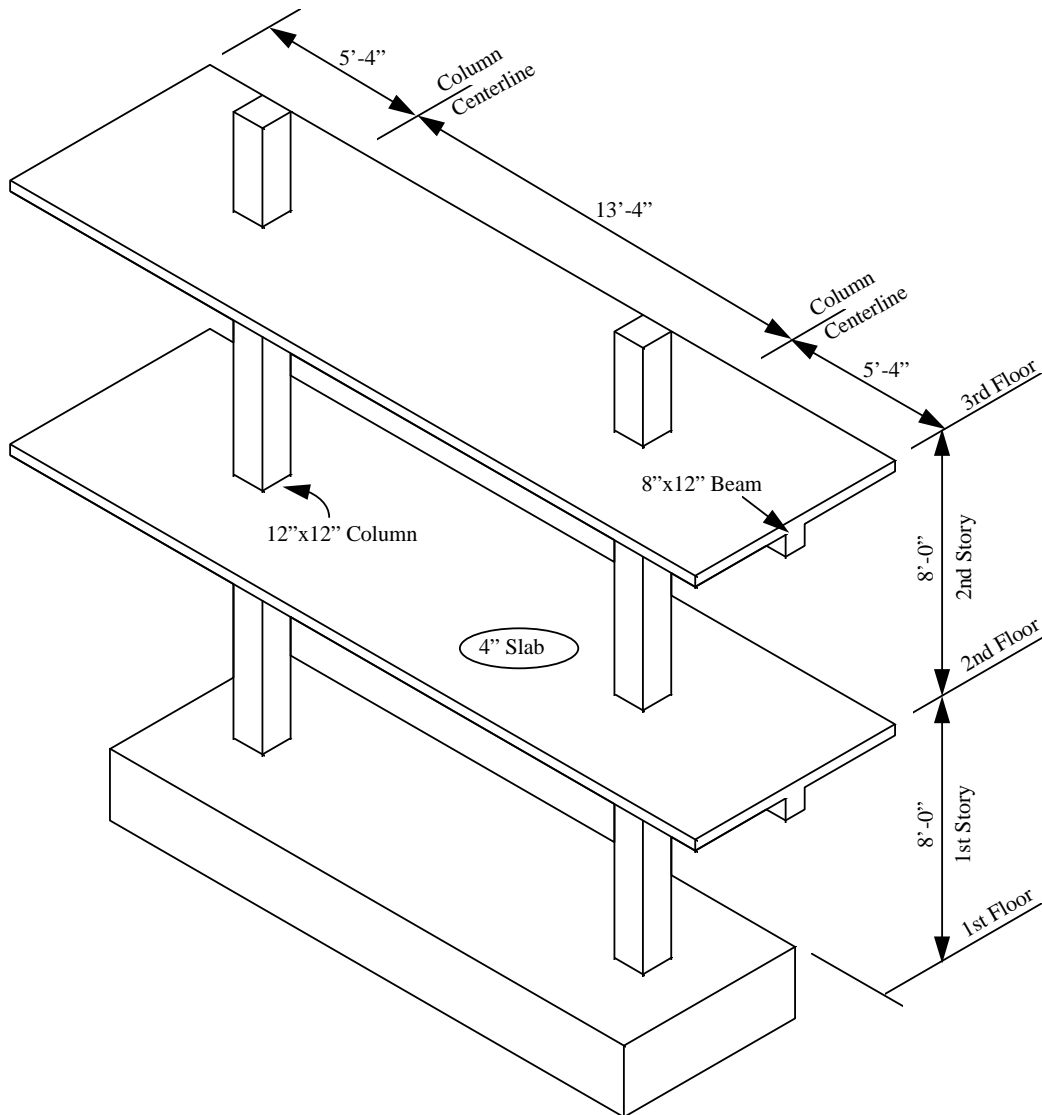


Figure 2.2: Existing Frame of Test Structure^[6]

- *Column Splices.* Longitudinal column bars are spliced just above the floor levels. These splices were designed as compression splices only, with a lap length of 15 in. ($20 d_b$) for #6 bars.
- *Column Ties.* The 12 in. square columns are reinforced with #3 ties with 90° bends, spaced at 12 in.
- *Beam Reinforcement.* Positive moment reinforcement is discontinuous through the beam-column joints, with a 4 in. embedment length into the column. Similarly, negative moment reinforcement was discontinuous in the midspan region where positive moment controls design. Finally, U-shaped stirrups are used for shear reinforcement, and are discontinued in the middle third of the span.

Figure 2.3 shows a detail of a beam-column joint as constructed in the test specimen, depicting many of the above problems.

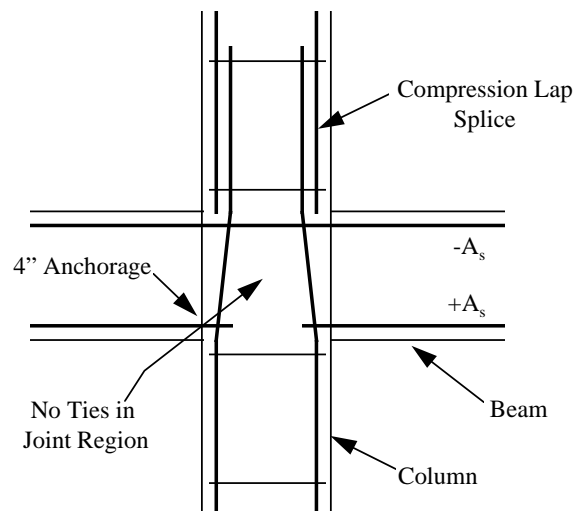


Figure 2.3: Beam-Column Joint in Test Specimen^[6]

The specimen was designed to be loaded at the 2nd and 3rd floor levels, using the floor slabs as diaphragms to transfer shear to the frame. Loads were designed to be taken out at the base by attaching the frame to a base block footing anchored to the strong floor of the laboratory. The geometry of the footing was chosen to position the frame portion of the structure conveniently for attachment of loading devices from the strong wall to the frame at the floor levels.

2.2.3 Construction

The existing frame model was cast in place in four stages, beginning with the base block footing, followed by each story, and concluding with the column stubs on top.

Figure 2.4 shows the pre-pour condition of the footing structure. Post-tensioning bar anchorages for the infill system were provided by casting bars with anchor plates into the footing. These bars extended above the top of the footing to allow for other bars to be spliced later using threaded couplers. Column bars were anchored via 90° hooked ends cast in the footing.

During construction, the formwork for the floors and beams was shored to the ground using wooden two-by-fours and four-by-fours. The two columns below a floor level were cast simultaneously with that floor. Figures 2.5 through 2.8 show various stages in the construction of the model frame from the first story to the completed structure.

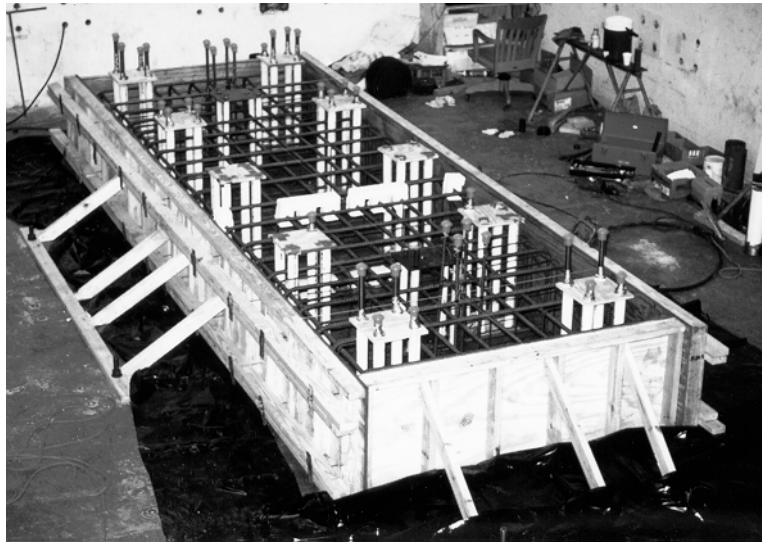


Figure 2.4: Footing Construction



Figure 2.5: First Story Construction



Figure 2.6: Completed First Story



Figure 2.7: Second Story Construction



Figure 2.8: Completed Existing Frame

2.3 Connection Tests

In order to achieve monolithic behavior in a wall system composed of precast elements, two types of connections are critical to the design. First, the panels must be connected to each other ("panel connection"). Second, the panels must be connected to the frame ("frame connection"). Prior to installing an infill wall in the existing frame, a series of tests (phases I & II) were performed to investigate the design and behavior of these key connections.

2.3.1 Panel Connection Tests

Figure 2.9 shows a panel connection test component and its representative location in the infill wall. Fourteen specimens of panel connection components were constructed. The specimens were loaded in reversed cyclical direct shear across the horizontal interface between the panels and the grout strip. Thus, the tests performed do not simulate actual forces encountered by the connection within a shear wall, but they do allow for comparison of the effects of different variables involved in construction of the joint.

The main results investigated were peak strength and residual strength. Three basic factors in the construction of the connection contribute to component

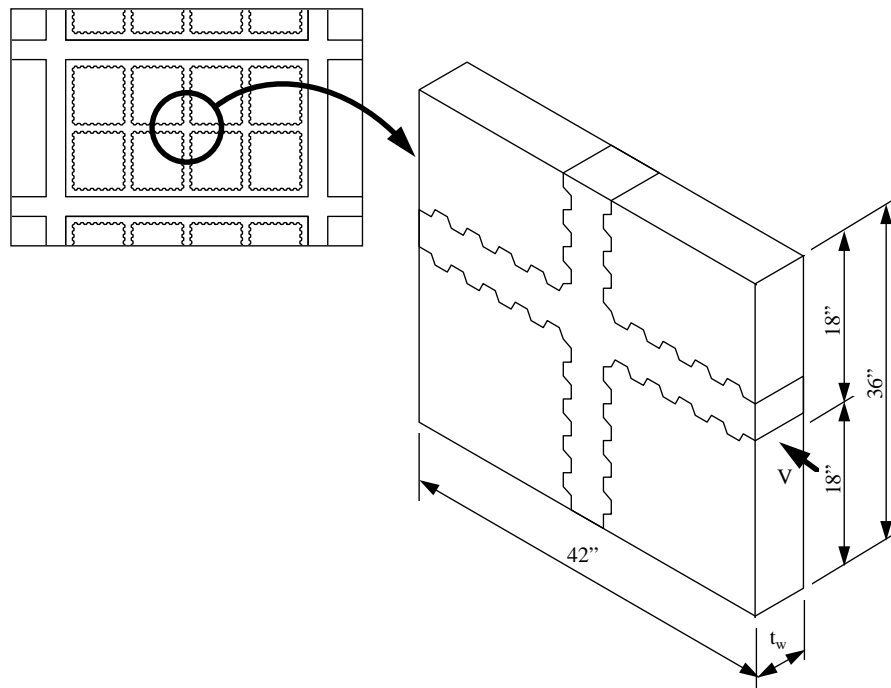


Figure 2.9: Panel Connection Specimen^[6]

strength and shear transfer across the interface to form a monolithic connection. First, the panels themselves are reinforced with welded wire fabric (two layers of 4x4 W2.9 x W2.9). Second, shear keys are used on the perimeter of the panels to transfer forces from the panels to the grout strip. Based on previous investigations of shear keys, the geometry of the keys was chosen to cause a shear failure along the base of the key before overriding or dislocation occurs. Third, reinforcement is provided in the grout strip (closure strip) between the panels. Once the shear keys fail across a horizontal plane, the vertical reinforcement in the closure strip enables shear friction to develop across the interface. Horizontal reinforcement was included in the component construction, although it has no direct contribution to shear transfer in these tests. In an actual wall in a structure, horizontal reinforcement is required by ACI^[3] detailing criteria, so it was included in these tests to model actual field conditions in the joint. The details of a typical panel connection specimen are illustrated in Figure 2.10.

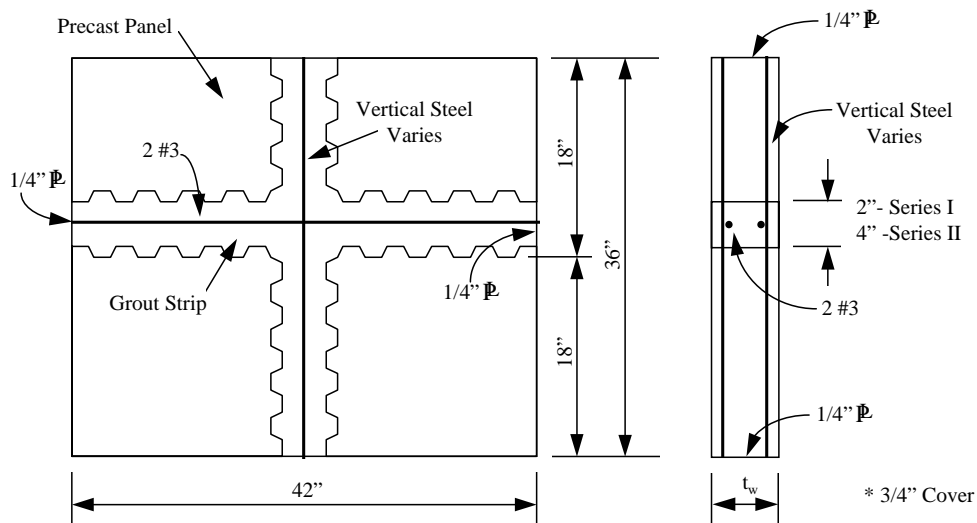


Figure 2.10: Panel Connection Details^[6]

2.3.1.1 Test Variables

Variables investigated in the panel-to-panel connection tests include:

- *Shear key configuration.* The effect of the alignment of the shear keys on one panel with respect to the keys on another panel was investigated. The keys were either aligned or staggered (see Figure 2.11a). In addition, the spacing of the keys was varied. The two spacings studied were full spacing and 1.5-spacing. The fully spaced keys were separated by a valley distance equal to the dimension of the peak, and the 1.5-spaced keys were separated by a valley distance of 1.5 times the peak dimension. The spacings of the keys are shown in Figure 2.11b.
- *Shear key size.* Two key sizes were used, one being 1.5 times the size of the other. The proportions of the keys were kept geometrically similar, as shown in Figure 2.11c.
- *Panel spacing.* The test specimens were constructed using panel-to-panel clear spacings of 2 in. and 4 in.
- *Vertical steel.* The effect of vertical reinforcement in the closure strip was studied, with reinforcement amounts ranging from two-#3's to six-#5's.
- *Grout strength.* To determine the effect of the strength of the grout material relative to that of the panels, grout strength was varied. Panel material strengths were kept constant, while both stronger and weaker grout was used in the closure strips.
- *Panel thickness.* Two panel thicknesses, 4 in. and 6 in., were investigated. It is likely that for different rehabilitation projects, different wall thicknesses will be convenient.

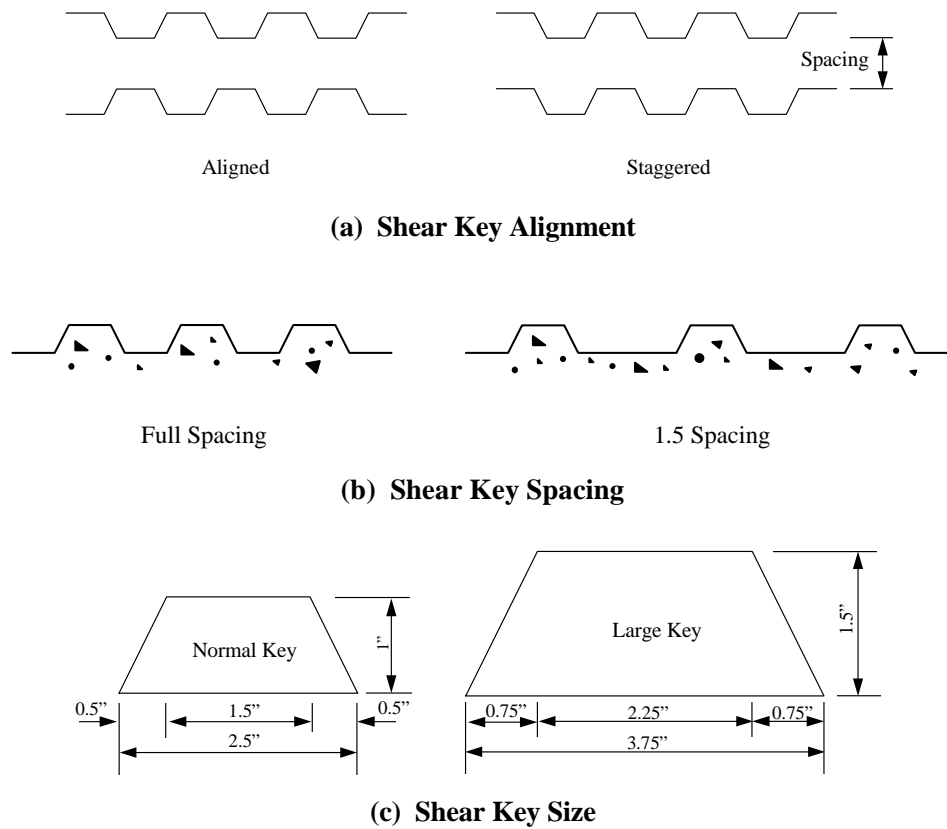


Figure 2.11: Panel Connection Test Variables^[6]

2.3.1.2 Results

A typical load-displacement response curve from these panel connection tests is presented in Figure 2.12. As can be observed in this plot, the progression of strength development for these specimens was:

- *Adhesion capacity.* Initially, the specimen is very stiff, until adhesion is broken along the interface between the panel shear keys and the grout.

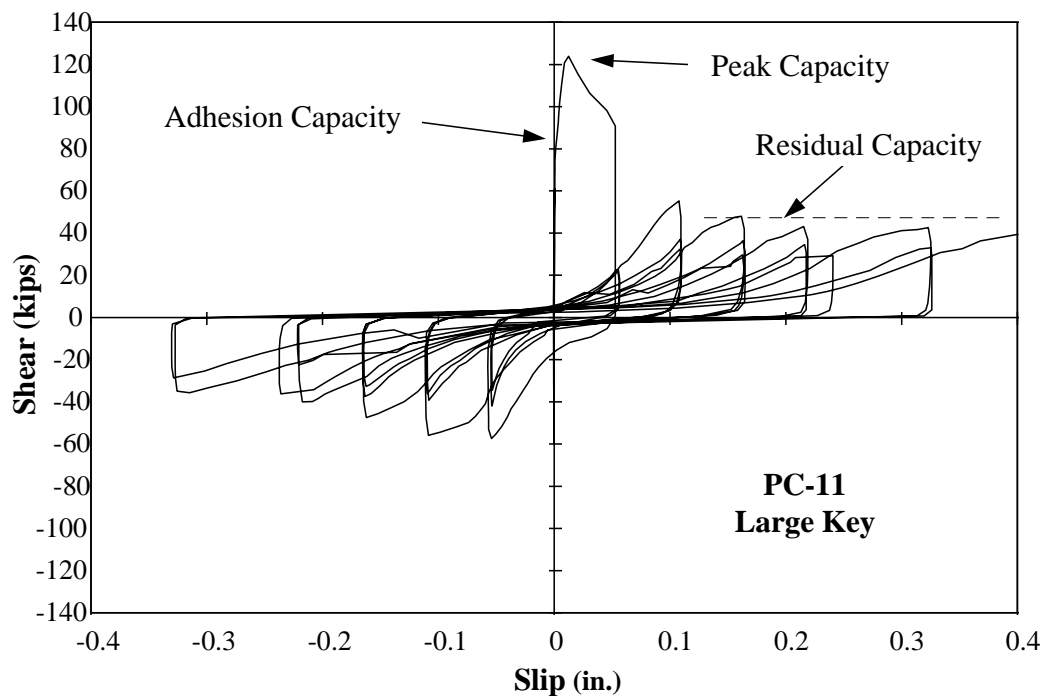


Figure 2.12: Typical Panel Connection Test Results^[6]

- *Peak capacity.* After loss of adhesion, some stiffness is lost, but the load continues to increase until the peak capacity is reached when a failure plane develops along the shear keys.
- *Residual capacity.* After the shear keys fail, the vertical reinforcement in the closure strip is mobilized in shear friction and yields, creating a ductile failure mechanism with a residual strength typically between 30% and 40% of the peak strength.

It should be noted that adhesion loss does not always occur. The shear keys can fail before adhesion loss occurs, resulting in only a peak capacity and residual capacity for a connection.

Based on the results of these tests, it was determined that the most important variables which contribute to the strength of the connection are grout strength (which influences peak strength), vertical reinforcement (which influences both peak strength and residual strength), and panel thickness (which influences both peak strength and residual strength).^[6]

2.3.2 Frame Connection Tests

A similar series of tests was performed to investigate the connection of the panels to the existing frame. Figure 2.13 shows a frame connection test component and its representative location in the infill wall. Four specimens were constructed and tested in a manner similar to the panel connection specimens.

The main difference in the construction of a frame connection specimen is the use of a steel tube as a shear lug across the interface. A small number of steel pipes in the precast infill wall system take the place of numerous interface dowels used in cast-in-place methods. New variables were included in this series of tests, while most variables from the panel connection series of tests were kept constant. The details of the frame connection specimen are illustrated in Figure 2.14. Normal size, aligned keys were used at full spacing. The panels were spaced 4 in. apart, and a 4 in. separation was used between the panels and the frame element. The grout strength was higher than that of the panels in each of the tests.

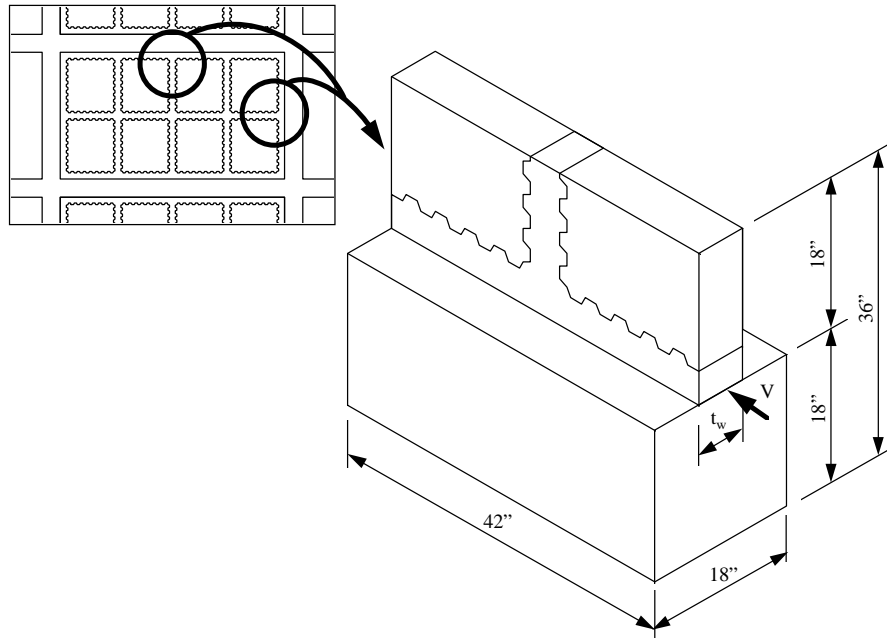


Figure 2.13: Frame Connection Specimen^[6]

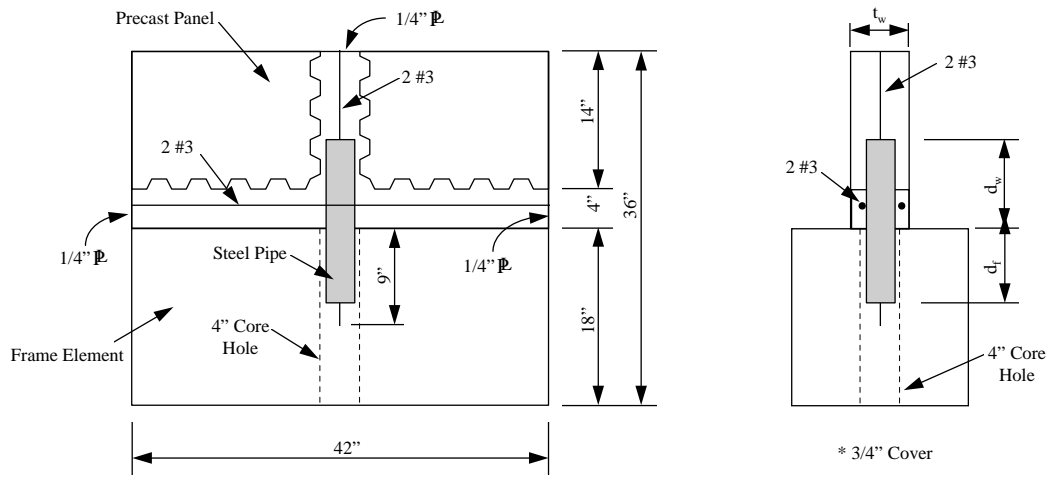


Figure 2.14: Frame Connection Details^[6]

2.3.2.1 Test Variables

Variables in the Frame Connection tests include:

- *Panel thickness.* Three tests were performed using 6 in. panels, and one test was performed using 4 in. panels.
- *Steel pipe embedment length.* The embedment of the pipe into the frame and between the panels was varied from 4 in. to 9 in. Embedment lengths were chosen based on the ACI^[3] bearing strength area required to develop yield strength of the pipe.
- *Steel pipe size.* For the three specimens with 6 in. panels, a 2-1/2 in. diameter extra-strong pipe was used. For the specimen with 4 in. panels, a 2 in. diameter extra strong pipe was used. These pipe sizes were chosen based on the maximum dimension allowed by the geometry of the specimen (panel width).

2.3.2.2 Results

The specimens behaved similarly to the panel connection specimens, as can be seen in Figure 2.15. After adhesion loss, capacity increased at a reduced stiffness until the shear keys failed, after which residual capacity was developed by shear friction. From these tests, it was determined that the connection is adequate to mobilize the strength of the panels. The steel pipe should have enough embedment length to develop residual strength (i.e., it should extend through the grout strip into the space between the panels), or else the connection should be designed based on satisfactory vertical reinforcing steel, as in the panel connection tests.

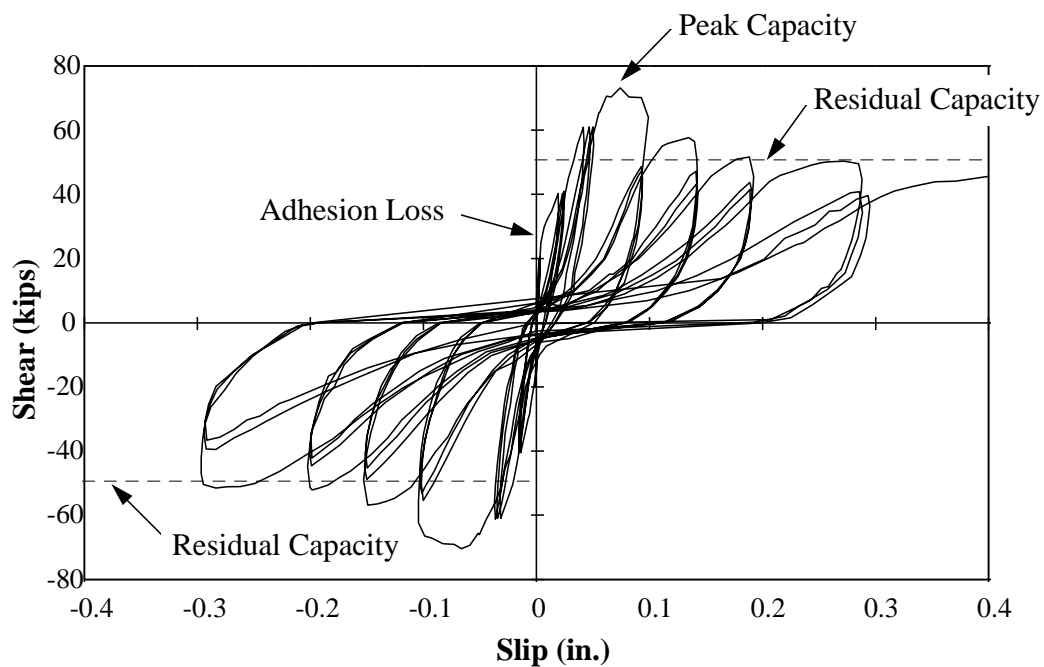


Figure 2.15: Typical Frame Connection Test Results^[6]

2.4 Infill Wall

The next step in the research program (phase III) was to use the information from the connection tests to construct an infill wall system to fill the existing frame model. The general layout of panels is shown in Figure 2.16. Two rows of panels were used at each floor level, with four panels in each row, making a total of sixteen panels for the two-story existing frame. This layout was chosen so that the panels were a convenient size for handling, while as few panels as possible were required to fill a bay. This layout also allows space for several shear lugs (steel pipes) to be used to connect the wall to the frame. In this layout, three lugs each are used at the top and bottom of the wall, while one lug is used on either side at midheight of the columns.

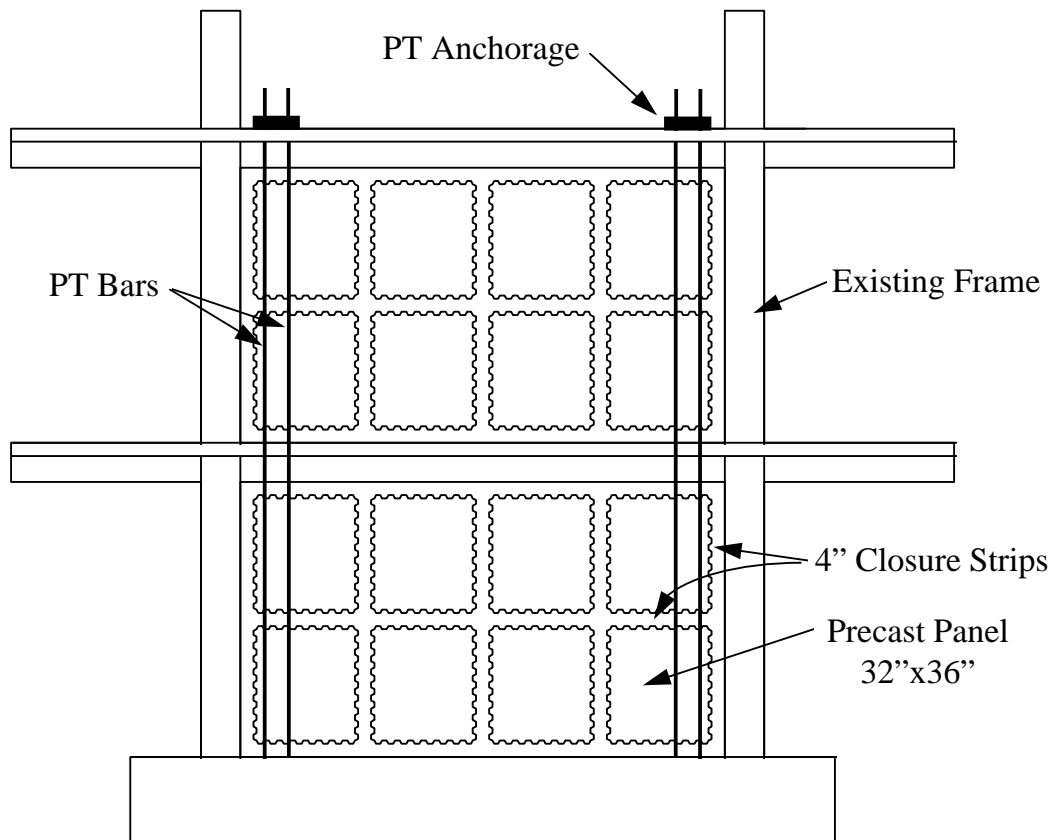


Figure 2.16: Infill Wall Installed in Original Frame^[6]

The goal of the construction was to provide for monolithic behavior of the wall, and the intent of the design was to have sufficient shear capacity to permit flexural hinging at the base of the wall via yielding of external post-tensioning bars installed adjacent to the existing columns. Because the column splices are not expected to be able to develop ductile yielding, they are not relied on in this system.

2.4.1 Infill Wall Construction

The construction of the infill wall proceeded in three stages. First, the panels were cast. Second, the panels were placed in the structure one row at a time and grouted into place in four stages. Finally, the external post-tensioning bars were installed and anchored. Figure 2.16 illustrates the model existing frame with an infill wall installed.

The panels were cast flat in wood forms, similar to the procedure performed in creating the panels for the connection tests. Two layers of 4x4 W2.9 x W2.9 welded wire fabric were used in the panels with a cover of 3/4 in. The strength of the panels was designed to be greater than that of the shear lugs of the frame connection. Based on the results of the panel connection tests, normal size shear keys were used in the aligned configuration with normal spacing. A set of 6 in. panels and a set of 4 in. panels were cast for the first and second floors, respectively. Figure 2.17 shows the formwork for the panels prior to casting. In addition to reinforcing steel, two lifting inserts were attached to each side of the

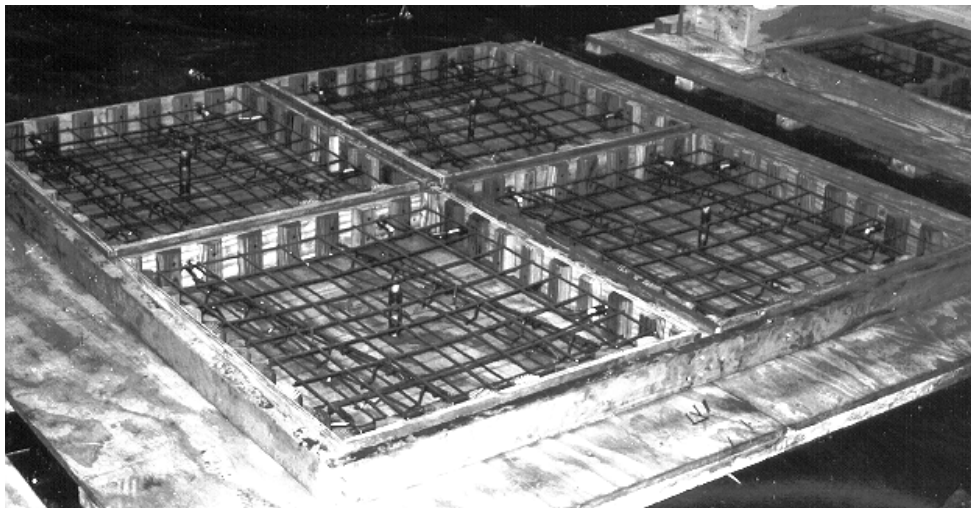


Figure 2.17: Precast Panel Formwork and Reinforcement

forms, and two more inserts were placed at the center of the panel. These inserts later aided in the handling, placement, spacing, alignment and bracing of the panels in the structure.

Once the panels were cast, preparations were made in the frame for insertion of the panels. The holes for the shear lugs had been cast into the existing frame using PVC pipe to void the space, but some of these pipes shifted during casting. A coring machine was employed to re-cut holes to the proper depth or at the correct location. All of these holes would have to be cored in an existing structure. Before this is done, however, it is important to locate steel reinforcement in the columns and beams before coring. In the beams, it is likely that some of the steel will have to be cut, so temporary shoring may be required during construction.

The panels were placed in four stages, as shown in Figure 2.18. The panels were brought to the structure and lifted to the proper floor using a light forklift. Due to space restrictions at the floor levels, the forklift could not be used to place the panels. Instead, a 2-ton crane, supported from the story above, was used to place the panels using clevis plates bolted to the lifting inserts at the top or sides of the panels (Figure 2.19). In the inserts not occupied by clevis plates, bolts were inserted to help space the panels 4 inches apart. Once in place and aligned with the aid of the bolts, plywood panels were bolted to the lifting inserts at the front and back centers of the panels, and two-by-fours were nailed to the plywood to brace the panels to the floor (Figure 2.20). Afterwards, the vertical and horizontal strip steel could be placed, along with the steel pipes (Figure 2.21). Four #4 bars were used in the 6 in. wall, while three #4 bars were placed in the 4 in. wall. The amounts of steel were chosen so that the connections would be stronger than the strength of the shear lugs. For the 6 in. wall, a 2-1/2" diameter XS pipe was used, while a 2" diameter XS pipe was used in the 4 in. wall. These

pipes were sized so that a flexural failure of the wall system should occur before a shear failure.

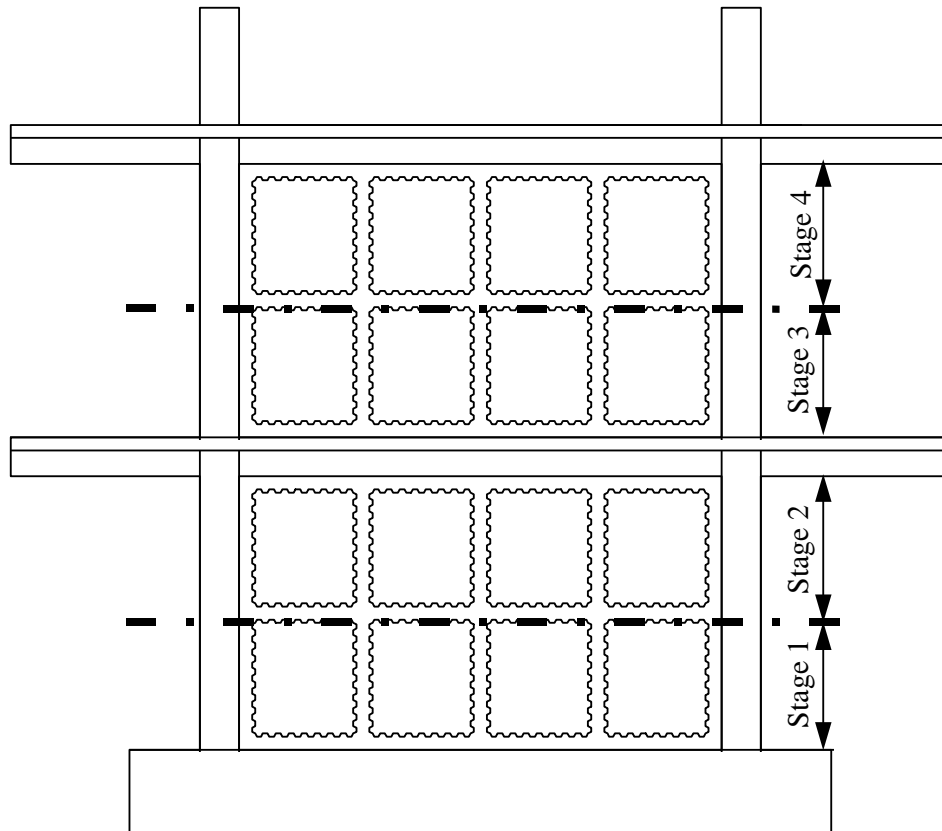


Figure 2.18: Infill Construction Sequence^[6]



Figure 2.19: Crane Used for Panel Placement

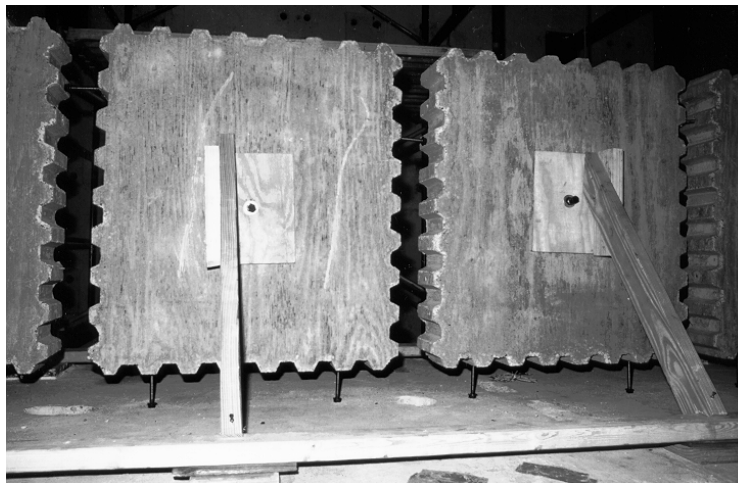


Figure 2.20: Panel Placement Using Inserts and Braces

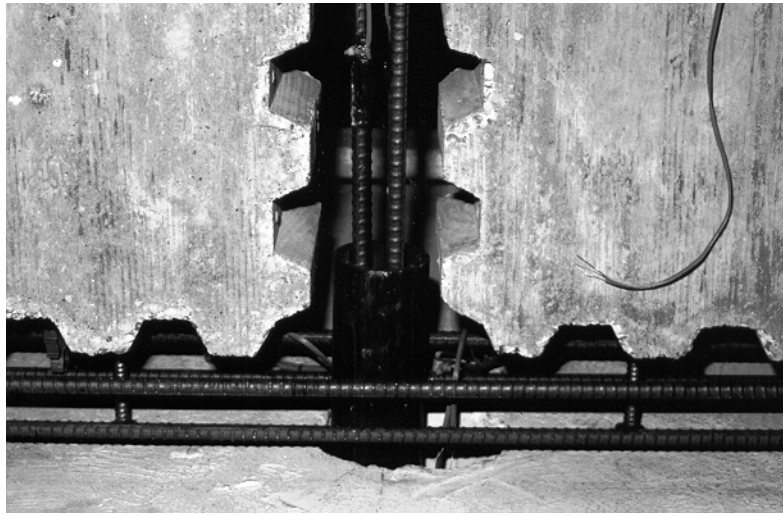


Figure 2.21: Rebar and Pipe Placement

Upon completion of panel and steel placement, the closure strips (gaps between adjacent panels and between the panels and the frame) were closed with plywood forms held in place with snap ties. The formed closure strips are shown in Figure 2.22. On one side, access holes had been cut out of the forms to allow a vibrator to be inserted into the closure strips during grouting. A flowable grout mix with small aggregate and an 8 to 10 in. slump was scooped into the forms, and moved using a combination of hydrostatic pressure and vibration. Figure 2.23 shows the grouting operation for an upper level of panels, where grout was poured in through the core holes and vibrated from the floor above, while workers below vibrated the mix through access holes.

The last step in the infill construction process was to install the post-tensioning bars. Bars were spliced approximately 12 in. above each floor level using threaded couplers. The bars were left unbonded over their entire length, and were anchored at the top of the structure using steel plates and nuts. The bars were inserted through the top of the structure and brought down to the appropriate

level. Alternatively, the bars could have been inserted at each floor level, provided that the holes in the floors are large enough to permit angling of the bars during insertion. For tests in which post-tensioning force was applied to the bars, a pair of 60-ton hydraulic rams were brought to the top of the structure. These rams were pressurized simultaneously on two adjacent bars to avoid inducing out-of-plane moments on the wall.

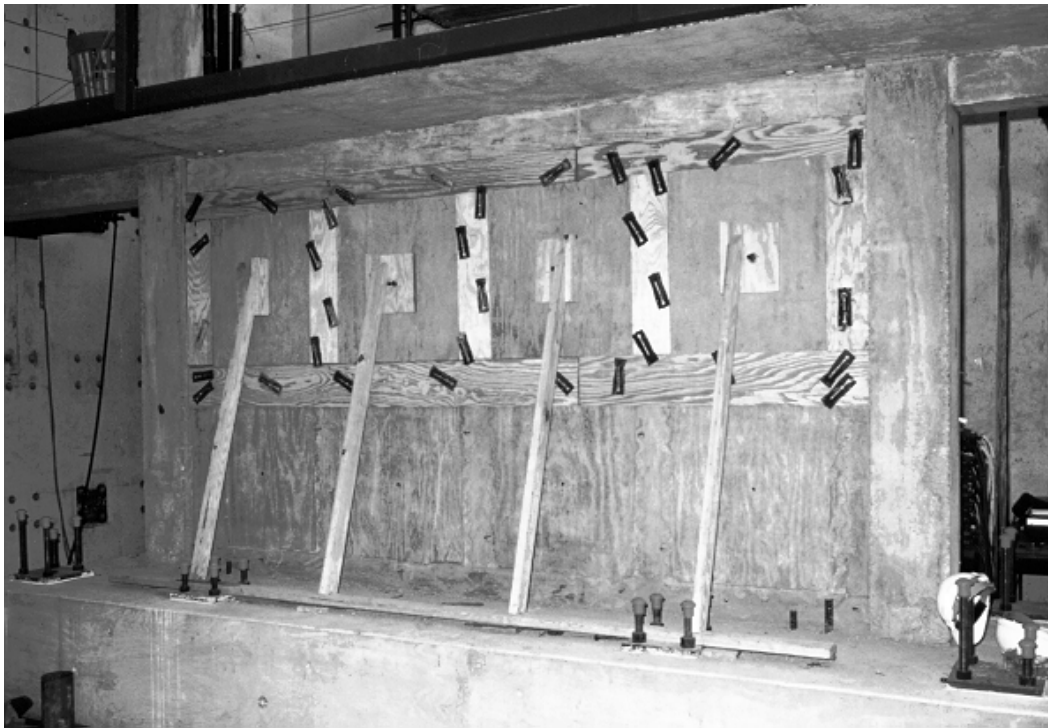
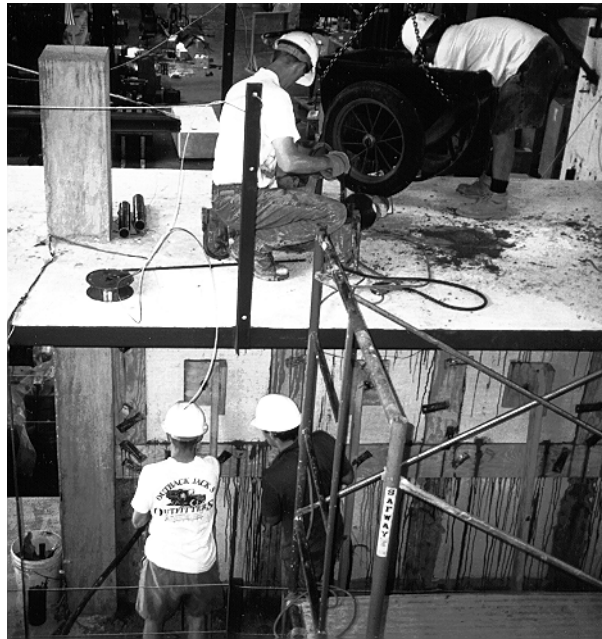


Figure 2.22: Closure Strips Formed for Casting Stage 2



**Figure 2.23: Panel Casting Operation
During Casting Stage 4**

2.5 Removal of Infill Panels

To study the effects of openings on the behavior of the infill wall system, selected panels were removed in succession from the wall after tests had been conducted on the full infill.

The panels were removed in two stages corresponding to the two tests that were performed on the infill with openings. First, an interior panel on the upper row of the first story wall was removed, creating a “window”. After tests were performed on the structure, two vertically aligned panels were removed from the second story wall to create a “door”, and a second series of tests was performed.

The single panel from the lower level was cut along the grout strip using a large gas-powered circular concrete saw with a water wash coolant. Figure 2.24

illustrates the sawing operation. The cuts were made just inside the boundary of the shear keys of the panel so that the panel keys remained in the wall. Cuts were made from both sides of the wall to cut as much of the perimeter as possible without over-cutting into the remaining portion of the wall. This process left small portions of the panel attached to the wall at the corners, so the panel had to be knocked out of the wall using a sledge hammer. Figure 2.25 shows the wall with the panel removed.

Because the wall on the upper level is thinner than that of the lower level, it was possible to cut the two panels out of the wall with a less powerful saw. A hand-held circular saw with an abrasive blade was employed for this process. Once again, the cut was made just inside the panel boundary and from both sides of the wall. At the bottom of the opening, the horizontal grout strip was also removed using a jack hammer to prevent shear transfer across the opening through the strip. The wall with the "door" opening is shown in Figure 2.26.



Figure 2.24: Panel Sawing Operation

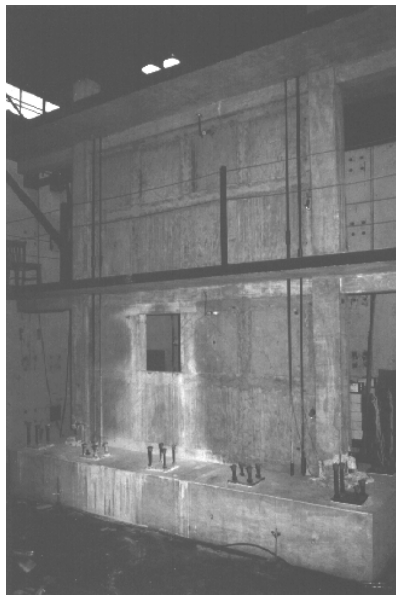


Figure 2.25: Wall with Window

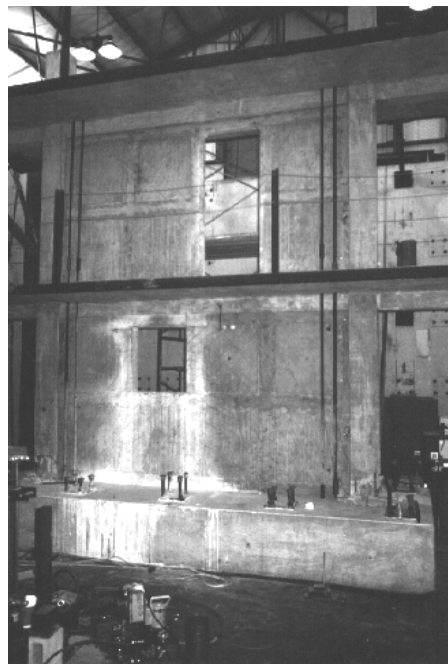


Figure 2.26: Wall with Doorway at Second Level

2.6 Material Data

2.6.1 Concrete

The concrete used in the construction of the existing frame had a nominal design strength of 3000 psi. This strength reflects the relatively low-strength concrete typically used in construction in the 1950's and '60's. For the precast infill panels a nominal strength mix of 4000 psi was chosen because this is more common for above-grade structural elements in contemporary construction. Finally, a 6000 psi concrete mix was selected for the closure strips in order for them to be stronger than the panels.

The base footing was constructed with 3/4" maximum size coarse aggregate, while the concrete in the frame, precast panels, and closure strips used 3/8" aggregate to satisfy clear spacing and cover requirements. The frame and panel batches were adjusted at the laboratory to attain a 6 in. slump. The closure strip concrete was adjusted with water at the laboratory to attain a 6 in. slump, then superplasticizer was added to bring the slump to between 8 and 10 inches. Mix proportions and slump data for all concrete used in the specimen are shown in Table 2.1. Exact proportions as delivered in the ready-mix truck varied slightly.

The precast panels were cast in two sets of eight (four 6 in. and four 4 in.) panels apiece. The second group of panels to be cast became the lower row of panels in each story, while the first set became the upper row in each story. The closure strips were cast in four stages, as described in Section 2.4.1.

Standard 6 in. by 12 in. cylinders were employed to monitor the strength gain of each cast of concrete. For each of the concrete batches except the footing batch, sets of three cylinders were tested at 7, 14, and 28 days, as well as at the time of the full infill testing. The footing concrete strength was checked only at

the time of the full infill testing. Average compressive strengths for the concrete are shown in Table 2.2. Compressive strength of the footing concrete at the time of testing was 4600 psi.

Table 2.1: Concrete Mix Data

Material Data	Base Footing	Existing Frame	Precast Panels	Closure Strips
Cement ¹	360	400	470	693
Coarse Aggregate ¹	1884	1625	1625	1167
Fine Aggregate ¹	1435	1619	1655	1755
Water ¹	266	275	250	325
Admixture ²	10.5	12	20	27.6 ³
Max. Aggregate Size	3/4"	3/8"	3/8"	3/8"
Slump After Adjustment	6"	6"	6"	8"-10"

¹ Quantities given in pounds per cubic yard of concrete.

² Quantities given in ounces per cubic yard of concrete.

³ This number does not include 25 ounces of Superplasticizer per cubic yard of concrete added on-site to increase the slump.

Table 2.2: Concrete Compressive Strengths

Location	Compressive Strength (psi)		Age (days)
	@ 28 days	@ Test	@ Test
Frame: Second Floor	4024	4218	212
Frame: Third Floor	3617	3908	155
Panels: Lower Rows	5014	5297	128
Panels: Upper Rows	4210	4439	148
Closure Strip: Stage 1	6948	6914	49
Closure Strip: Stage 2	6916	7144	43
Closure Strip: Stage 3	6622	6700	40
Closure Strip: Stage 4	6626	6807	36

2.6.2 Steel Reinforcing Bars

Grade 60 reinforcing steel was used in the construction of both the existing frame and the infill wall. The welded wire fabric in the precast panels was also Grade 60. Representative coupons were taken from the shipments of steel to verify yield and ultimate tensile strengths of the reinforcement in tension. Testing was performed according to ASTM A370-94. Tensile yield and ultimate strength values for the reinforcement are given in Table 2.3. The welded wire fabric fractured at 72.2 ksi near the weld, and exhibited no yielding.

Table 2.3: Reinforcing Steel Properties

Steel	Yield (ksi)	Ultimate (ksi)
<i>Existing Frame</i>		
#5	61.3	99.9
#6	61.1	98.7
<i>Infill Wall Closure Strips</i>		
#4	63.0	102.8

2.6.3 Steel Pipes

The steel pipes used in the connection of the wall to the existing frame were ASTM A-53 Grade B. Coupons were removed from the pipes and tested according to ASTM A370-94 to determine tensile strengths. Yield and ultimate tensile strengths for the two sizes of pipe are given in Table 2.4. Note that the yield values are significantly higher than the specified minimum yield strength of 35 ksi for this grade of steel.

Table 2.4: Steel Pipe Properties

Pipe Size	Yield (ksi)	Ultimate (ksi)
2" Diameter XS	40.4	55.7
2-1/2" Diameter XS	53.6	71.6

The shear capacity of an individual pipe (V_n^{pipe}) can be determined by:

$$V_n^{pipe} = 0.6 A_s F_s$$

where A_s is the cross-sectional area of the pipe and F_s is the stress in the pipe.

Table 2.5 tabulates individual pipe shear capacities based on three stress levels.

Table 2.5: Individual Pipe Shear Capacities (in Kips)

Stress Level	2"- ϕ XS	2 1/2"- ϕ XS
Nominal Yield	31.1	47.3
Actual Yield	35.1	72.4
Ultimate	49.5	96.7

2.6.4 External Post-Tensioning Steel

Two sizes of Dywidag Grade 150 threaded bars, conforming to ASTM A722 Type II, were used as external post-tensioning steel in the specimen. These bars were tested for tensile strengths according to ASTM A370-94. Although these bars are of a high grade of steel, they exhibited excellent yield plateaus under testing. The results of the tests are given in Table 2.6.

Table 2.6: Post-Tensioning Steel Strengths

Nominal Bar Diameter (in.)	Nominal Area (in²)	Yield (ksi)	Ultimate (ksi)
1	0.85	152.9	170.6
1-1/4	1.25	146.0	160.4

2.7 Test Setup

2.7.1 Loading System

The loading system employed in this series of tests was used to simulate earthquake effects on the structure by applying cyclic loads to the structure in the plane of the wall. Four hydraulic rams capable of creating tension or compression forces were used to apply loads to the structure at the floor level as shown in Figure 2.27. Two 150 kip rams were used on the third floor (upper level), while two 100 kip rams were used at the second floor (lower level). These rams were attached to the reaction wall at buttressed locations. Each buttress can withstand 300 kips. The other ends of the rams were attached to loading heads located on either side of the slabs at the two floor levels. Each loading head is a system of steel plates which are welded to a steel angle located at the edge of the slab. These steel angles have shear studs distributed over their length, and were cast into the structure at the time the frame was constructed.

In the out-of-plane direction, the structure was braced against the reaction wall by two sets of double angles at each floor. The double angles were bolted to a plate attached to the reaction wall. Only one bolt was used in the connection of the angles to the wall to allow rotation of the angles in the plane of the floor.

Likewise, a single bolt attached the angles to a steel plate welded to the steel angle on the side of the floor slab.

The rams at the second and third floors were pumped independently to apply an inverted triangular load distribution over the height of the building. In other words, the load applied at the third floor was twice that of the second floor. This distribution simulates first mode of vibration effects, and is consistent with

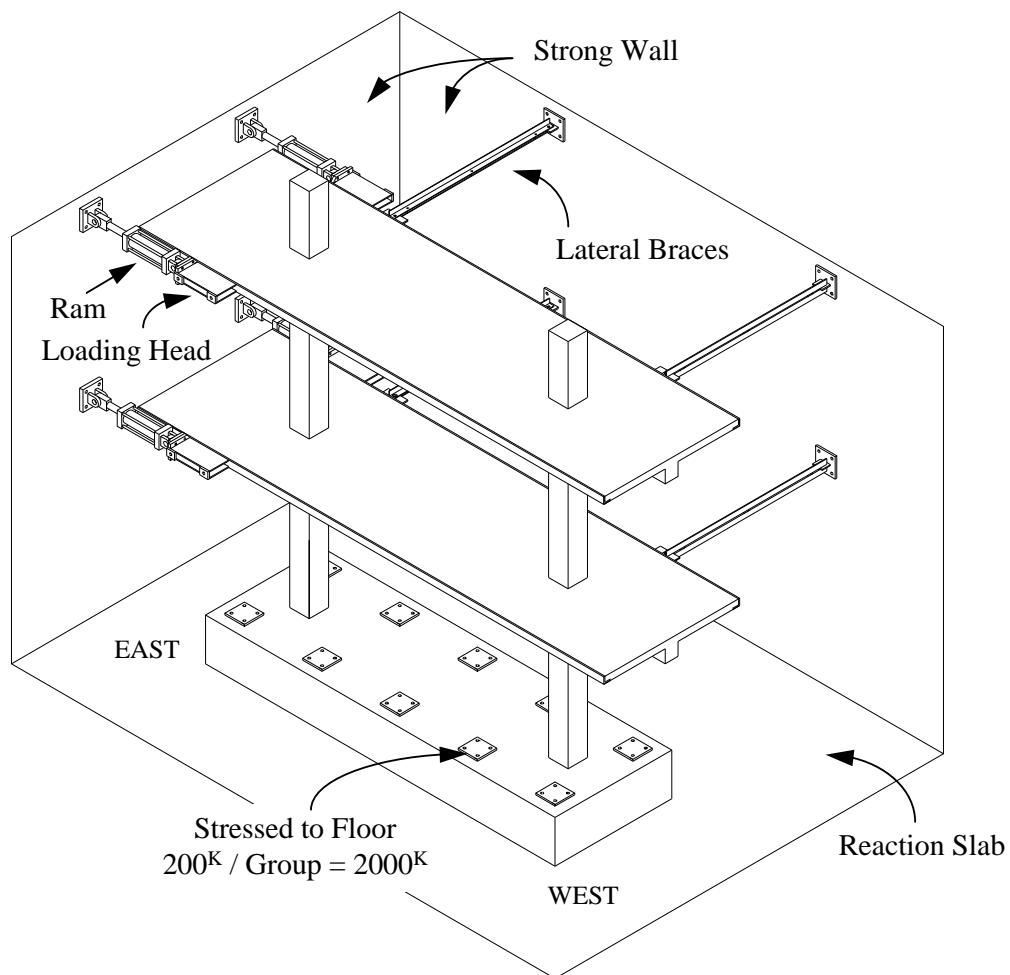


Figure 2.27: Test Setup^[6]

static-load design procedures in building code recommendations.^[4, 5, 11] The two

rams on a single floor were connected to a pressure manifold to equilibrate pressure in the rams. Due to slight differences in the internal friction of the rams, however, slightly different forces were generated in each ram. Loads were monitored in the rams via electronic shear pin load cells. Additionally, pressures in the rams were monitored with electronic pressure transducers and analog pressure gages.

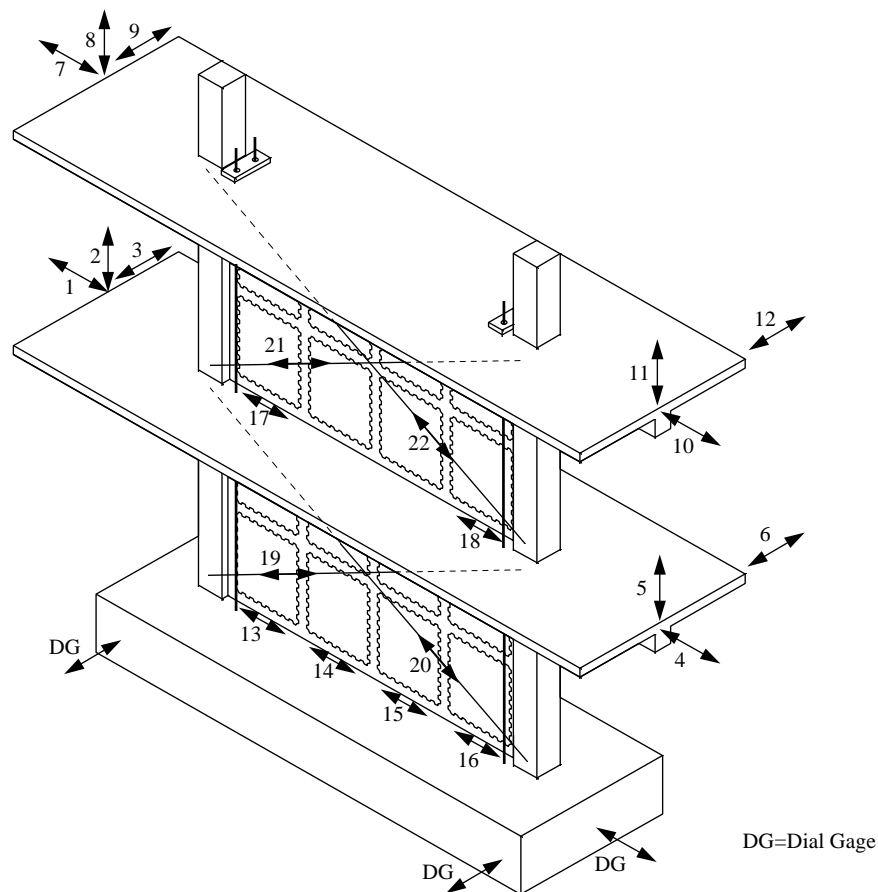


Figure 2.28: Displacement Gage Locations^[6]

2.7.2 Data Acquisition

Displacements of the structure and its parts were monitored with linear displacement transducers and dial gages, while strains in steel reinforcing bars and steel pipes were monitored with strain gages. The locations of these monitoring devices are shown in Figures 2.28 and 2.29. Two data acquisition systems were required to monitor the large number of load cells, transducers, and gages in the setup. The systems were separated into those devices monitoring action in the existing frame structure and those monitoring the infill wall.

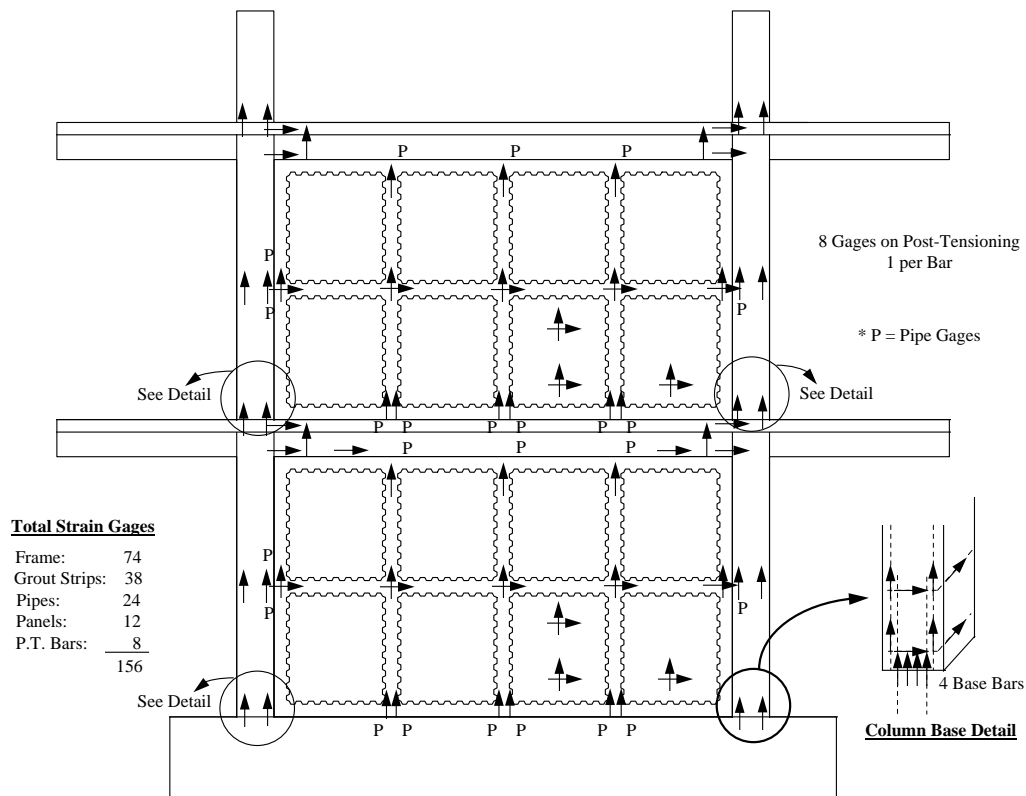


Figure 2.29: Strain Gage Locations^[6]

CHAPTER 2.....	6
2.1 INTRODUCTION	6
2.2 EXISTING FRAME	7
2.2.1 <i>Prototype Frame</i>	7
2.2.2 <i>Design and Details</i>	7
2.2.3 <i>Construction</i>	11
2.3 CONNECTION TESTS.....	14
2.3.1 <i>Panel Connection Tests</i>	15
2.3.1.1 Test Variables.....	17
2.3.1.2 Results	18
2.3.2 <i>Frame Connection Tests</i>	20
2.3.2.1 Test Variables.....	22
2.3.2.2 Results	22
2.4 INFILL WALL	23
2.4.1 <i>Infill Wall Construction</i>	25
2.5 REMOVAL OF INFILL PANELS	31
2.6 MATERIAL DATA	34
2.6.1 <i>Concrete</i>	34
2.6.2 <i>Steel Reinforcing Bars</i>	36
2.6.3 <i>Steel Pipes</i>	36
2.6.4 <i>External Post-Tensioning Steel</i>	37
2.7 TEST SETUP	38
2.7.1 <i>Loading System</i>	38
2.7.2 <i>Data Acquisition</i>	41
FIGURE 2. 1: TYPICAL 1950’S AND ‘60’S RC FRAME.....	8
FIGURE 2. 2: EXISTING FRAME OF TEST STRUCTURE	9
FIGURE 2. 3: BEAM-COLUMN JOINT IN TEST SPECIMEN	10

FIGURE 2. 4: FOOTING CONSTRUCTION.....	12
FIGURE 2. 5: FIRST STORY CONSTRUCTION	12
FIGURE 2. 6: COMPLETED FIRST STORY	13
FIGURE 2. 7: SECOND STORY CONSTRUCTION	13
FIGURE 2. 8: COMPLETED EXISTING FRAME	14
FIGURE 2. 9: PANEL CONNECTION SPECIMEN	15
FIGURE 2. 10: PANEL CONNECTION DETAILS.....	16
FIGURE 2. 11: PANEL CONNECTION TEST VARIABLES	18
FIGURE 2. 12: TYPICAL PANEL CONNECTION TEST RESULTS.....	19
FIGURE 2. 13: FRAME CONNECTION SPECIMEN.....	21
FIGURE 2. 14: FRAME CONNECTION DETAILS	21
FIGURE 2. 15: TYPICAL FRAME CONNECTION TEST RESULTS	23
FIGURE 2. 16: INFILL WALL INSTALLED IN ORIGINAL FRAME	24
FIGURE 2. 17: PRECAST PANEL FORMWORK AND REINFORCING.....	25
FIGURE 2. 18: INFILL CONSTRUCTION SEQUENCE.....	27
FIGURE 2. 19: CRANE USED FOR PANEL PLACEMENT	28
FIGURE 2. 20: PANEL PLACEMENT USING INSERTS AND BRACES.....	28
FIGURE 2. 21: REBAR AND PIPE PLACEMENT	29
FIGURE 2. 22: CLOSURE STRIPS FORMED FOR CASTING STAGE 2.....	30
FIGURE 2. 23: PANEL CASTING OPERATION DURING CASTING STAGE 4.....	31
FIGURE 2. 24: PANEL SAWING OPERATION	32
FIGURE 2. 25: WALL WITH WINDOW	33
FIGURE 2. 26: WALL WITH DOORWAY AT SECOND LEVEL.....	33
FIGURE 2. 27: TEST SETUP.....	39
FIGURE 2. 28: DISPLACEMENT GAGE LOCATIONS.....	40
FIGURE 2. 29: STRAIN GAGE LOCATIONS	41
TABLE 2. 1: CONCRETE MIX DATA	35
TABLE 2. 2: CONCRETE COMPRESSIVE STRENGTHS	35
TABLE 2. 3: REINFORCING STEEL PROPERTIES.....	36
TABLE 2. 4: STEEL PIPE PROPERTIES.....	37

TABLE 2. 5: INDIVIDUAL PIPE SHEAR CAPACITIES 37
TABLE 2. 6: POST-TENSIONING STEEL STRENGTHS 38

CHAPTER 3

SPECIMEN HISTORY AND PRE-TEST CONDITION

3.1 Introduction

Before the structure was tested with panels removed to determine the effects of openings on the infill wall's behavior (hereafter these tests are referred to as "window and door tests"), a series of three tests was performed on the same specimen. This chapter outlines the performance of the structure in these tests, and describes the damage incurred during testing. This review is intended to give the reader an idea of the performance of the full infill, as well as the pre-test condition of the specimen prior to the experiments which are the focus of this paper. For a full report on the original frame and full infill wall tests, see Reference 6.

The next three sections (3.2 through 3.4) of this chapter describe the three sets of tests performed on the specimen prior to the window and door tests: (1) bare existing frame test, (2) full infill flexure test, and (3) full infill shear tests. Each section briefly describes the intent of the test, load history, performance, and damage incurred. Section 3.5 describes repairs performed on the loading system as a result of damage incurred during the shear tests. The final section (Section 3.6) summarizes the condition of the structure prior to the window and door tests.

3.2 Bare Existing Frame Test

Before the infill wall was constructed, the bare nonductile existing frame was loaded to evaluate its performance and anticipated weaknesses. Typically,

existing structures are cracked due to loads encountered during their service lives, so introducing damage to the model frame prior to adding the infill wall reflects expected conditions in the field.

The structure was subjected to cyclic lateral loads from the rams at the floor levels. The maximum base shear applied during these tests was 10 kips: approximately 6.7 kips at the third floor and 3.3 kips at the second floor, in keeping with the inverted triangular load distribution described in Chapter 2.

3.2.1 Performance

Two main problem areas prevented the structure from being able to safely carry higher loads. First, a pullout failure of the positive moment beam bars from the face of the column at the second floor appeared imminent. If these bars had failed, forces in the structure would have been redistributed, causing an increase in tension forces on the upload column. This increase would have triggered the second problem: a failure of the lap splices for the longitudinal column reinforcement, and would have formed a collapse mechanism for the structure. The behavior of the existing frame closely followed expected events from analysis. Based on this performance, seismic rehabilitation of a similarly constructed structure would be recommended.

3.2.2 Damage

No major damage was allowed to occur in the frame due to the risk of collapse associated with overloads. The damage incurred in the bare frame test was flexural in nature and could be predicted with fair accuracy by frame analysis. In the columns, cracks formed at the bases of the columns on floors 1 and 2, as well as at the soffits of the beams at beam-column joints. Otherwise, the

columns remained uncracked. Flexural cracking in the beams and floor slabs occurred at the beam-column joints at both floors. Additional cracks occurred along the length of the beam on the second floor.

3.3 Full Infill Flexure Test

After the existing frame test, the infill wall was constructed. At this point, only two (out of four possible) post-tensioning bars were installed at each end of the wall. These bars were used because the design shear strength of the infill indicated that a flexural failure (yielding of the post-tensioning bars) could not be obtained if more bars were installed on each side (accommodations had been made to install a total of four bars at each end). Near the east column, two 1 in. Dywidag bars were installed, while two 1-1/4 in. bars were installed near the west column. This was done to observe the difference in behavior based on the two different areas of tensile steel. A total of 108.1 kips of tension was applied to the east bars and 129.1 kips to the west bars. The intent of this test was to fail the column splices and then achieve a flexural failure at the base of the wall by yielding the post-tensioning bars.

The maximum base shear applied during this test was approximately 275 kips. The load distribution in this test, as with all other tests, was an inverted triangle, with the load at the third floor being twice that of the second. After the splices failed in the east column at approximately 255 kips base shear, the load was released and then cycled to drift level intervals in the same direction that splice failure occurred (the west direction). The maximum drift of the structure during this test was about 0.575%.

3.3.1 Performance

Initially, the structure was very stiff, until the initial compression induced by the post-tensioning bars was overcome. At this point, termed the "decompression load," the stiffness gradually decreased. In the west direction (forces applied to the west), a splice failure was achieved in the east column, and the stiffness of the structure decreased further. Figure 3.1 illustrates the behavior of the specimen prior to splice failure, and Figure 3.2 shows the load-displacement history for the entire test. Subsequent cycles in the west direction revealed an initially higher stiffness due to compression in the post-tensioning bars, followed by a reduction in stiffness upon exceeding the decompression load. It was observed that the initial forces in the post-tensioning bars helped pull the structure back to near its original position upon release of the loads. At large drift levels, yielding occurred in one of the two 1 in. bars. Loads were not applied to fail the splice in the east direction, because the base shear was approaching the design shear capacity.

The overall performance of the wall was excellent in this test. The wall greatly increased the stiffness and strength of the structure, while developing a ductile flexural failure mechanism.

3.3.2 Damage

Some damage of significance occurred in the full infill flexure test. Flexural cracking appeared at regular intervals along the height of the columns in the first story. When the splices in the east column approached failure, vertical splitting cracks became noticeable in the splice region. As mentioned in the

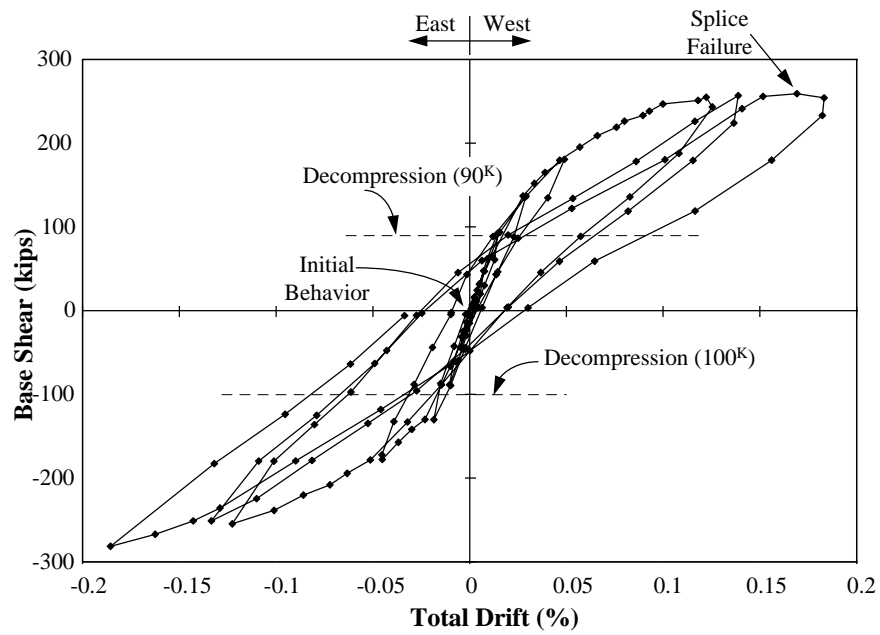


Figure 3.1: Behavior of Full Infill Prior to Splice Failure During Flexure Test^[6]

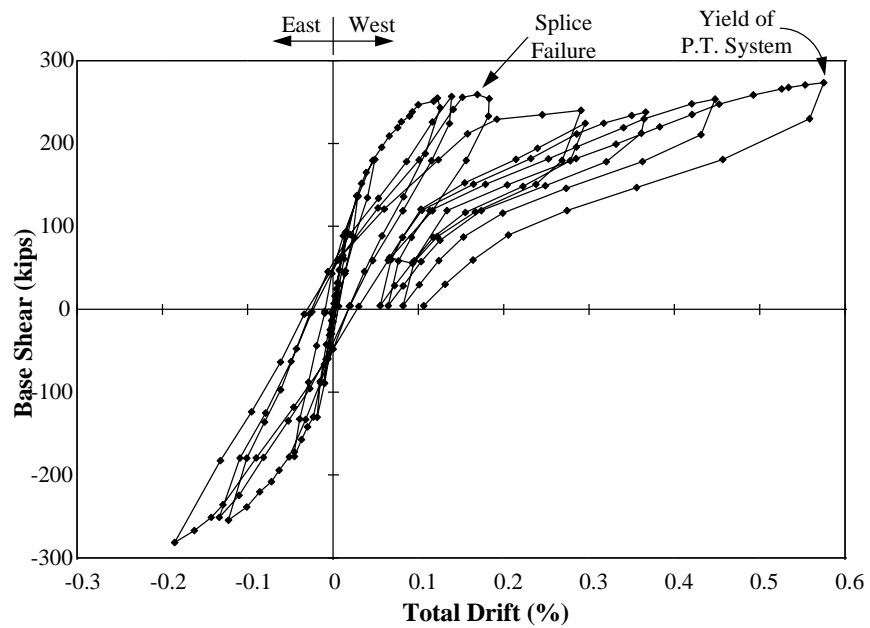


Figure 3.2: Behavior of Full Infill Wall During Flexure Test^[6]

previous section, the splices in the east column failed, causing a reduction in the stiffness of the structure. After splice failure occurred in the east column and uplift forces were taken primarily by the post-tensioning bars, the wall began to rotate as a rigid body at the base of the wall. This rotation occurred about the corner of the wall at the end opposite of the tension bars. The rotation of the wall produced a large gap, measuring up to $3/4$ of an inch, between the base of the wall and the top of the footing at the east end. With unloading, the gap closed completely. Because the post-tensioning bars were unbonded, the only flexural crack that formed in the wall was at the base.

The first shear cracks appeared in the wall at a base shear of about 250 kips. Many of these shear cracks were located on a diagonal line from the toe of the wall to the post-tensioning bar anchorage at the opposite end of the wall. A secondary line of cracks was located on a diagonal from the toe of the wall to the opposite corner of the wall at the second floor. The cracks propagated through panels and grout strips, indicating that the components of the wall had been successfully connected to achieve monolithic behavior. The wall crack pattern is pictured in Figure 3.3

Shear cracks form perpendicular to lines of principal tension. The line of a crack indicates a line of principal compression. Therefore, shear cracks can help identify major compression struts in a wall. From Figure 3.3, two main compression struts are identifiable, which are illustrated in Figure 3.4. Load paths, as indicated by compression struts, can be of particular importance if a panel along a major path is removed, as is the case in the window and door tests.

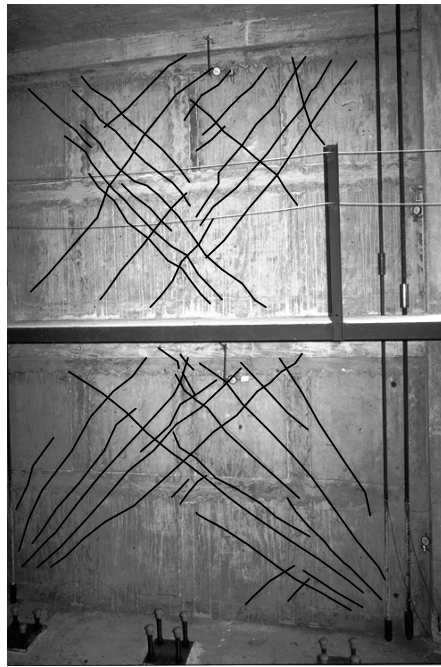


Figure 3.3: Cracking Pattern in the Full Infill Wall

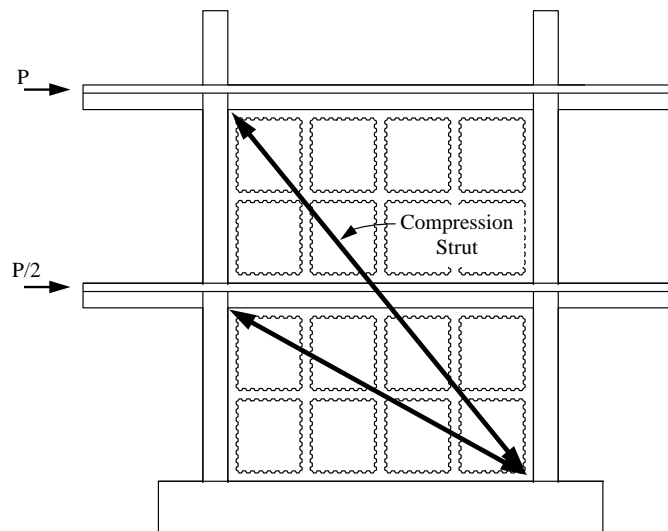


Figure 3.4: Main Compression Struts in Full Infill^[6]

3.4 Full Infill Shear Tests

Upon demonstrating that a ductile flexural failure mechanism is possible with this construction, two tests were performed to fail the wall in shear. For these tests, two more 1 in. Dywidag bars were installed at each end of the wall. The additional steel was intended to increase the flexural capacity of the wall so that a shear failure would occur before the bars yielded. In the first shear test, just over 500 kips of total post-tensioning was applied to the eight bars. Before a shear failure could be attained in this test, however, the capacity of the loading system was reached. Thus, a second test was performed without any post-tensioning force applied. Since compression forces increased the shear strength of the wall, it was reasoned that releasing the post-tensioning forces would enable the wall to fail in shear and provide a lower bound on the shear strength of the system. For the second shear test, the post-tensioning forces on the bars were released, and the bars were anchored with the nuts in a snug-tight position.

Initially, the loads on the structure were cycled back and forth at base shears of approximately 270 and 360 kips. Because the splices in only the east column (corresponding to loading in the west direction) had failed in the flexure test, the structure was stiffer in the east direction. The next loading in the east direction produced a splice failure in the west column at 421 kips. After splice failure, the load was increased to 450 kips, with a slight change in stiffness. Two full cycles to 450 kips of base shear were performed, until a failure in the loading system occurred in the west direction. The details of the loading system failure and the repairs required for the window and door tests will be discussed in Section 3.5. At this point, the test with initial tension in the rods was stopped. The load-drift record for this test is shown in Figure 3.5.

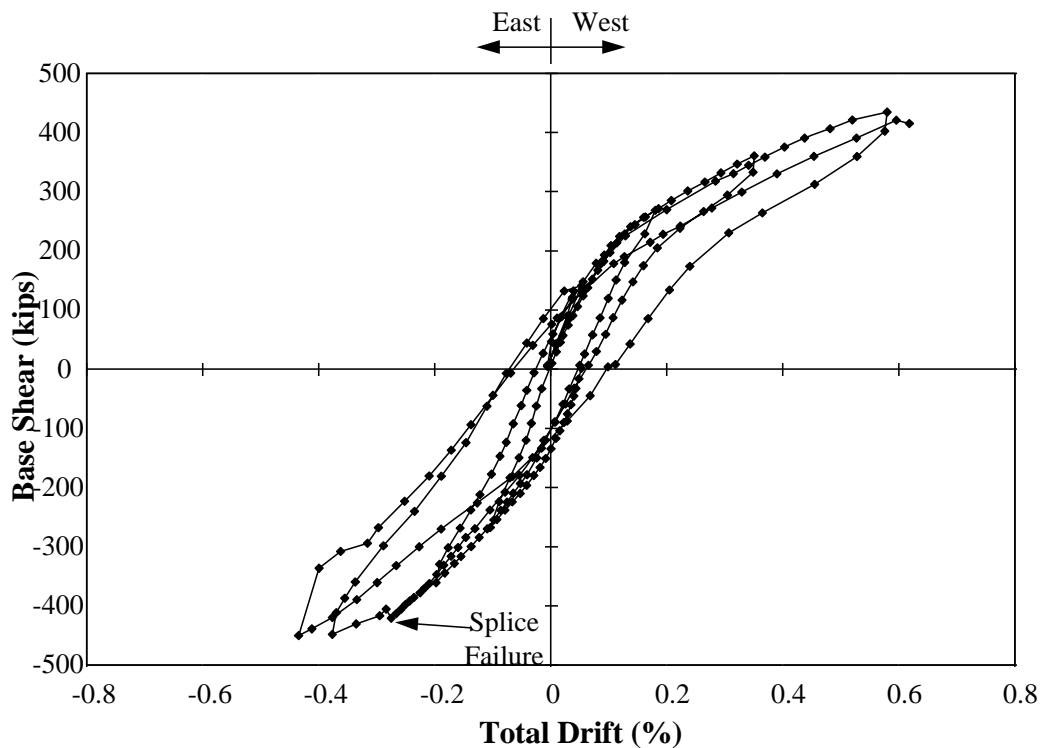


Figure 3.5: Behavior of Full Infill During First Shear Test^[6]

After detensioning the rods, testing continued. Although the loading system had failed in the west direction, load could still be safely applied to the structure in the east direction. To estimate the lower bound shear capacity of the wall, the structure was loaded monotonically in the east direction. The maximum base shear reached during this test was 491 kips. Figure 3.6 shows the load-drift record for this test.

3.4.1 Performance

Up to approximately 300 kips base shear, the structure maintained its initial stiffness. Beyond that load, the stiffness began to decay gradually as extensive shear cracking occurred and existing cracks continued to grow. At

about 460 kips base shear, a distinct change in stiffness was noted. At the maximum base shear of 491 kips, spalling occurred in the main compression strut near the top of the structure. As before, the main compression strut was located on a diagonal line from the toe of the wall at the download (east) column to the post-tensioning anchorage location at the top of the opposite (west) side. The spalling occurred in the horizontal grout strip immediately below the soffit of the existing frame beam. Based on the low stiffness of the structure in the last phase of loading, together with the spalling of the concrete, it is likely that the wall had neared its shear capacity.

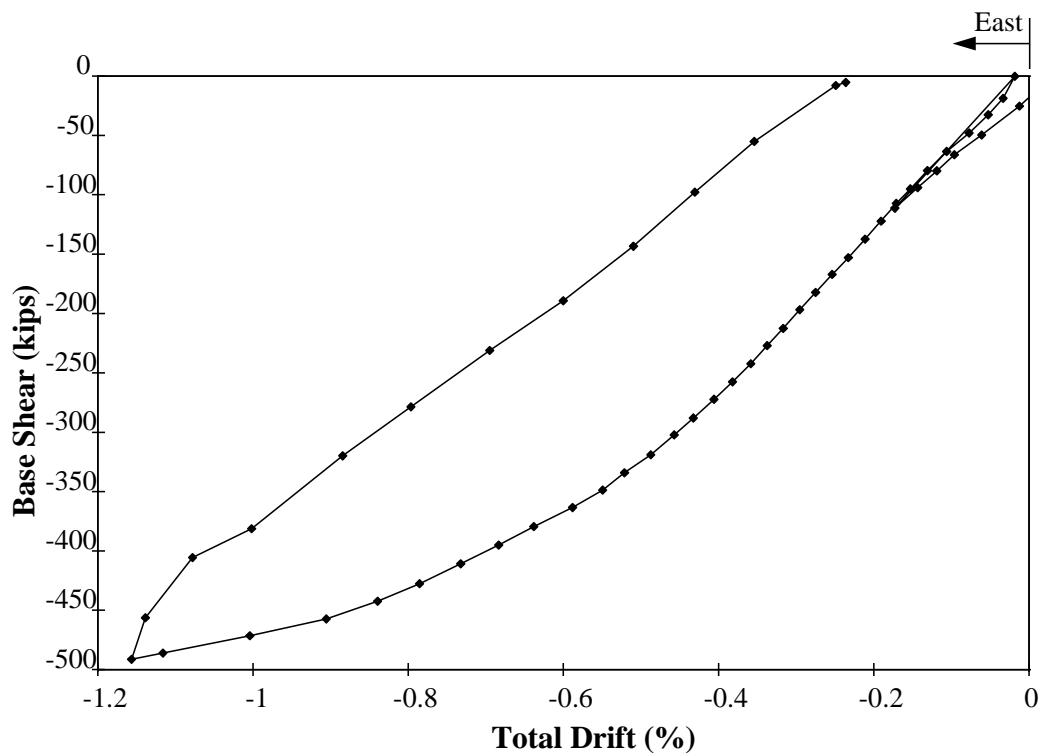


Figure 3.6: Behavior of Specimen During Final Shear Test^[6]

3.4.2 Damage

As mentioned above, the column bar splices failed in the west column during these tests; however, it was still possible to increase the load in the structure due to the presence of the post-tensioning bars. Many shear cracks formed along compression struts, resulting in a gradually decaying stiffness. Slight spalling had begun to occur in the horizontal grout strip at the top edge of the wall. Further damage was prevented because the load was released and not cycled once the damage initiated. Very little concrete was lost at this location, leaving most of the bearing material in place for the shear lugs. Damage in the wall panels themselves was limited to controlled shear cracking.

3.5 Damage and Repairs to the Loading System

The last loading in the west direction during the shear tests created a failure in the loading system. The damage, shown in Figure 3.7, was the result of uplift on the slab at the third floor. Because the wall was rotating as a rigid body about the toe of the wall at the west column, large vertical displacements occurred on the east side of the structure. Uplift of the specimen caused the rams to tilt upward, creating a vertical force component which increased with increased loading. In turn, this vertical force component produced uplift on the floor slabs, which cantilever out from the wall in the north and south directions. These uplift forces became great enough to produce a flexural failure in the slab at the southeast corner. The failure line extended in an arc from the west end of the loading head to the eastern edge of the slab along the cantilevered beam. The brittle tensile failure (fracture) of the welded wire fabric which reinforced the slab allowed a brittle failure of the slab. Yielding of the steel angle occurred on the

west side of the loading head, on the line of the failure arc. This yielding helped slow the failure of the slab, although the slab still failed with little warning.



Figure 3.7: Failed Loading System at Third Floor, Viewed From the Southwest

Because the angle yielded, a permanent upward deformation remained in the slab. As a result, it was decided that load could no longer be applied in the west direction because any force from the ram would simply create more uplift force. Load could still be applied in the east direction because those forces served to straighten the loading system. When east direction loads were released, the slab returned to its post-failure position.

Thus, in order to be able to apply forces in both directions for the window and door tests, the structure required retrofitting. Two tasks were required for

this operation: first, the slab needed to be pulled down so that the load would come into the structure with a minimal (initial) vertical component; second, a brace needed to be attached to the slab to prevent the slab from returning to its post-failure position once it was released.

The slab was pulled down using the south hydraulic ram from the second floor. The ram was left attached to the wall, but detached from the loading head on the second floor. The ram was then tilted upward and the free end was connected to the loading head at the third level via a steel angle tension member. Next, the ram was used to pull the slab down to a horizontal position. The ram remained loaded until a bracing system could be installed.

Several options for bracing the slab were considered. It was decided that the best place from which to brace the slab would be the second floor east column. Had the brace been tied to the second floor, uplift forces would simply have been transferred to that floor, creating the possibility of a failure there. Tying the slab to the strong floor below would have prevented the slab from being able to rise with the wall as it rotated, creating the possibility of downward forces on the slab. By tying the slab to the column, the slab was allowed to rise with the structure as the wall rotated, while being prevented from deflecting in flexure.

The retrofit was performed with available materials at the lab. The installed brace (a 2" diameter XS pipe) spanned from the southeast corner of the slab to the east face of the east column, about 24 in. above the second floor. Holes were cored in the corner of the slab, and two 1 in. thick steel plates were bolted together through the holes in the slab. A gusset plate was welded to the plate which hung underneath the slab, and the brace was attached to the gusset plate with a single bolt. The other end of the brace was attached to a gusset plate which was welded to another steel plate. The steel plate was attached to the

column with four expansion anchor bolts. The connection of the bracing system to the column is pictured in Figure 3.8.



Figure 3.8: Connection of Bracing System to Column

To prevent a similar collapse from occurring in the third floor loading system on the other (north) edge of the slab, another brace was similarly installed, connecting the northeast corner of the slab to the column. A steel angle was used for this brace, shown in Figure 3.9.



Figure 3.9: Brace for the Loading System

3.6 Condition of the Specimen

This section summarizes the damage that had occurred in the tests prior to the window and door tests. Although some damage had occurred, the basic load transfer mechanism of the infill wall system remained intact. Diagonal compression struts had formed, but still had full capacity. Tension tie forces could be developed by the external post-tensioning bars.

The main damage that occurred was at the base of the columns on the first floor. The splices failed in both of these columns, causing extensive cracking and splitting in the lower 15 in. of the columns. Through repeated cycles of load in tension and compression, this region of the columns deteriorated until all the bars were exposed. Although some flexural cracking extended through the cores of the columns, the cores remained sound and capable of taking load in compression. Column splices would be likely to fail in a system of this type during an earthquake and thus cannot be relied on for uplift forces. Therefore, the door and window tests were not compromised by the fact that the column splices had already failed.

Rigid body rotation of the wall also caused the steel pipe shear lugs at the base to partially pull out during testing. When the loads were released, these pipes returned to their previous position. The embedment of the pipes in the frame was long enough to accommodate these vertical displacements without compromising their ability to transfer shear across the interface.

Shear cracking in the wall showed the development of compression struts as the tests progressed. These cracks remained relatively small (less than 0.8 mm wide) during the tests: new cracks would open before existing cracks widened significantly. Because the wall was adequately reinforced, the shear cracks did not reduce the capacity of the wall, but they did lead to decreased lateral stiffness of the overall system.

The damaged third floor slab was not repaired, but the modifications described in the previous section allowed the loading system to function properly during the window and door tests.

CHAPTER 3	42
3.1 INTRODUCTION	42
3.2 BARE EXISTING FRAME TEST	42
3.2.1 Performance	43
3.2.2 Damage.....	43
3.3 FULL INFILL FLEXURE TEST	44
3.3.1 Performance	45
3.3.2 Damage.....	45
3.4 FULL INFILL SHEAR TESTS.....	49
3.4.1 Performance	50
3.4.2 Damage.....	52
3.5 DAMAGE AND REPAIRS TO THE LOADING SYSTEM	52
3.6 CONDITION OF THE SPECIMEN	56
FIGURE 3. 1: BEHAVIOR OF FULL INFILL PRIOR TO SPLICE FAILURE DURING FLEXURE TEST.....	46
FIGURE 3. 2: BEHAVIOR OF FULL INFILL WALL DURING FLEXURE TEST	46
FIGURE 3. 3: CRACKING PATTERN IN THE FULL INFILL WALL	48
FIGURE 3. 4: MAIN COMPRESSION STRUTS IN FULL INFILL.....	48
FIGURE 3. 5: BEHAVIOR OF FULL INFILL DURING SHEAR TEST.....	50
FIGURE 3. 6: BEHAVIOR OF SPECIMEN DURING FINAL SHEAR TEST	51
FIGURE 3. 7: FAILED LOADING SYSTEM AT THIRD FLOOR, VIEWED FROM THE SOUTHWEST.....	53
FIGURE 3. 8: CONNECTION OF BRACING SYSTEM TO COLUMN	55
FIGURE 3. 9: BRACE FOR THE LOADING SYSTEM	56

CHAPTER 4

EXPERIMENTAL RESULTS

4.1 Introduction

The infill wall system was tested with selected panels removed to investigate the behavior of the system with openings in the wall, which are sometimes architecturally necessary or desirable. The structure was tested using cycled static loads at the floor levels. In the window test, the rams on both floors were used to produce high forces on the first story. In the door test, the top (third floor) rams were used to produce forces on the second story wall and the second floor rams were used to hold the second floor in place. The objective of these tests was to determine the effect of openings on the behavior of the infill wall system and to determine the force path in a system with openings.

No post-tensioning force was applied to the eight external Dywidag bars to simulate the conditions in the structure that existed during the prior test, the second shear test described in Section 3.4. The results can be more directly compared between the tests because the change in boundary conditions of the structure was kept to a minimum.

4.2 Window Test

4.2.1 Preliminary Observations on Panel Removal

The window panel was removed as described in Chapter 2. The removed panel was the second panel from the east end on the top row of panels in the first story. Figure 4.1 shows the cut-out panel prior to extraction from the wall,

viewed from the north. The diagonal lines on the panel are shear cracks that occurred during testing of the full infill. The cracks running from the upper left to the lower right formed during loading in the west direction; cracks running from the upper right to the lower left formed during loading in the east direction. Notice that there are many more cracks associated with east direction loading than west direction loading. It is apparent that the removed panel was more critical to compression strut formation for east loading than for west loading. It was therefore expected that east-direction loading would be more adversely affected by the opening than west-direction loading.

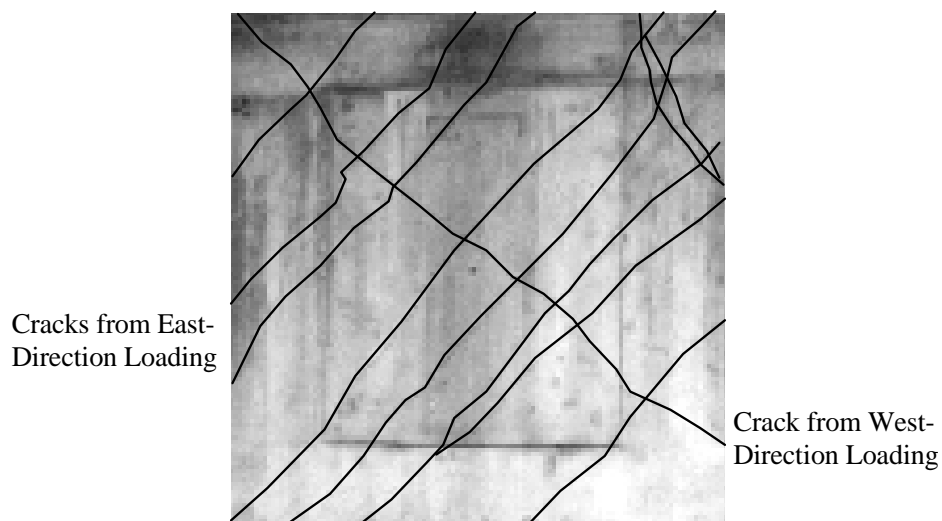


Figure 4.1: Cracks in Window Panel Prior to Removal

4.2.2 Structural Behavior

Two full cycles of load were applied to the specimen during the window test. The loading history is shown in Figure 4.2, and the load-drift response is presented in Figure 4.3. The first cycle reached a base shear of 150 kips, and

started in the west direction. The second cycle reached 300 kips in the west direction and nearly 450 kips in the east direction.

4.2.2.1 West Direction

In the early stages of loading in the west direction, up to approximately 150 kips base shear, no new cracks formed. At 150 kips some new small shear cracks began to form in the panel under the window, and in the panel directly to the right (west) of the window. Cracking increased gradually in the same areas up to the maximum applied forces. The cracks were generally on a line from the bottom left (east) corner of the window to the shear lug at the base to the right of the opening, indicating that the secondary compression strut that previously formed from the loading system at the second floor to the opposite toe of the wall was now developing below the window, and more force was being carried by the shear lugs at the base.

Although new cracking occurred during this test, the stiffness of the structure remained relatively constant throughout the test, indicating that the strength of the wall was being mobilized without significant new damage to the structure.

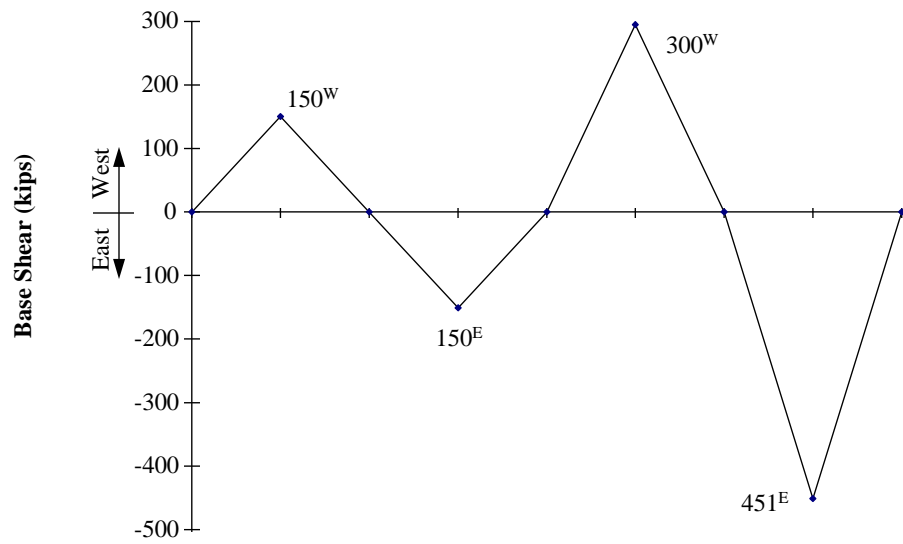


Figure 4.2: Window Test: Loading History

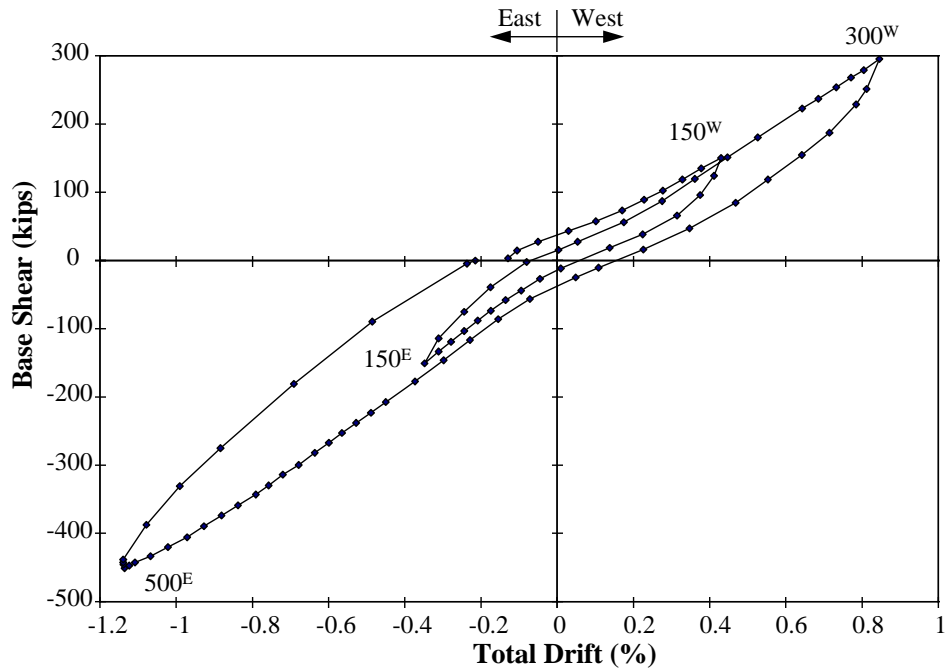


Figure 4.3: Window Test: Load vs. Drift Response

4.2.2.2 East Direction

At about 150 kips base shear in the east direction, existing cracks to the left (east) of the panel began to open. The main existing crack was along a diagonal from the upper left corner of the window to the left toe of the wall, and had not opened significantly before this stage. This indicated that this line of action was taking more force than it had previously, because the compression strut that previously formed through the window panel was now finding an alternate path above and around the opening. The middle shear lug at the opening effectively had no wall material to bear against, so the other two lugs had to carry a greater percentage of the load. New cracks parallel to the crack described above began to form in the two left panels at approximately 340 kips base shear. Existing cracks continued to open and extend toward the toe of the wall up to ultimate load. Damage and cracks which opened during east loading in the window test are shown in Figure 4.4. As in the previous tests with the full infill, cracks extended through grout strips, and the components of the system behaved together as a monolithic wall.

Above, on the second floor, new cracks opened in the second set of panels from the left (east), indicating that more load was being directed through the first shear lug to the left of the opening. One similar crack formed at 375 kips base shear at the shear lug on the right (west).

At 300 kips, crushing was observed at the toe of the wall. As loading continued, crushing of the compression zone (shown in Figure 4.5) increased, although no loss of stiffness was noted. At 375 kips base shear, it was observed that the wall was not rotating about the toe of the wall as it had in the previous tests. Instead, the base crack began to open at the middle of the wall at the central

shear lug, as shown in Figure 4.4. More downward thrust was probably directed to the first two shear lugs on the left due to the presence of the opening.

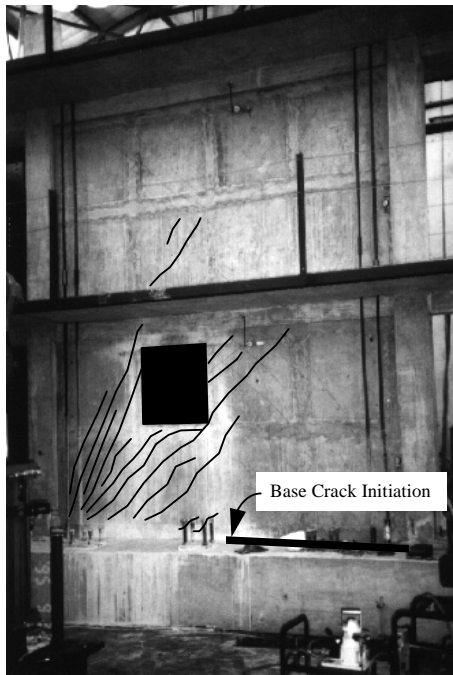


Figure 4.4: Damage During Window Test



Figure 4.5: Crushing at Toe of Wall

At approximately 300 kips base shear, new cracks began to form in the panel directly below the window. These cracks were directed from the bottom right (west) corner of the window to the first shear lug from the left (east) and the toe of the wall. The number of these cracks increased rapidly throughout the remainder of the test. As the structure reached its peak load of 450 kips, one crack along this line began to open dramatically (see Figure 4.6). With shear failure in the panel below the window and concurrent crushing of the toe of the wall, the structure resisted no additional load; peak capacity was reached.

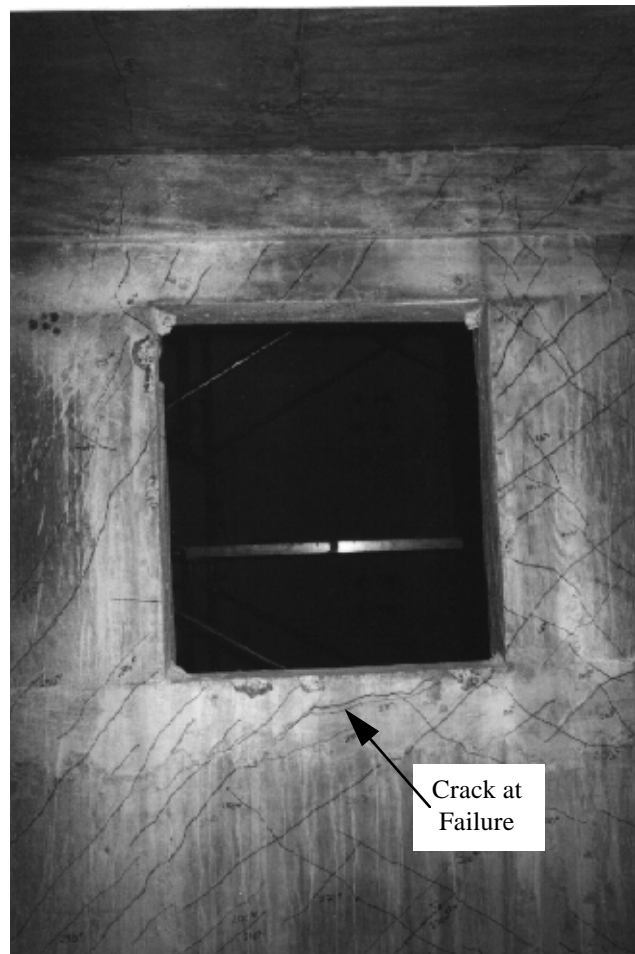


Figure 4.6: Cracking at Failure of Window Configuration

4.3 Door Test

4.3.1 Preliminary Observations on Panel Removal

After completion of the window test, the two panels were removed from the second floor, as described in Chapter 2. These panels were vertically aligned, creating a doorway in the wall, as shown in Figure 4.7. The removal of these two

panels created a discontinuity in the wall; load could no longer be transferred through the wall directly from one corner to the opposite one when loading in either direction. The only way for the load to be transferred across the opening was through the existing frame element above the door and the horizontal grout strip below the beam. For this test, the valves to the hydraulic loading system on the second floor were kept closed, and the structure was loaded through the third floor alone.

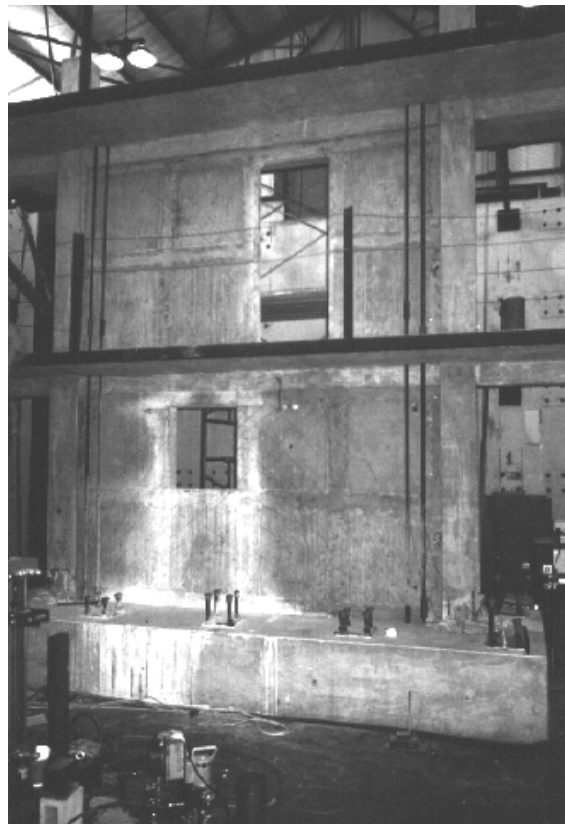


Figure 4.7: Door Configuration

4.3.2 Structural Behavior

Two-and-one-half load cycles were applied to the specimen during the door test. Figure 4.8 presents the loading history of this test, and Figure 4.9 shows the load-displacement response of the structure. Testing began in the west direction with a full cycle to 100 kips base shear (where “base” now refers to the base of the second story wall). The next west half-cycle went to 200 kips. Finally, the ultimate load was reached in half-cycles to 199 kips and 214 kips in the east and west directions, respectively.

4.3.2.1 West Direction

The first cycle in the west direction to 100 kips produced little new cracking in the structure. In the next cycle, to 200 kips, the structure maintained approximately the same stiffness as in the previous cycle, but the stiffness began to decrease slowly at about 140 kips. Shear cracks formed in the panels to the left (east) of the door on a diagonal from the upper left corner to the lower right corner. Diagonal cracks also formed in the panels to the right of the door, but these appeared to be primarily flexural-shear cracks in nature, as they started at the left edge of the wall and angled toward the toe. As loading continued, more flexural-shear cracks formed in higher portions of the wall. One existing shear crack in these two panels opened and extended during this cycle. The initiation of a shear failure was evident in the beam over the door as 200 kips was reached.

In the final cycle in the west direction, the structure responded at a slightly reduced stiffness (approximately 80% of its stiffness in the previous west cycle). This is probably due to the advanced failure of the coupling beam in the preceding

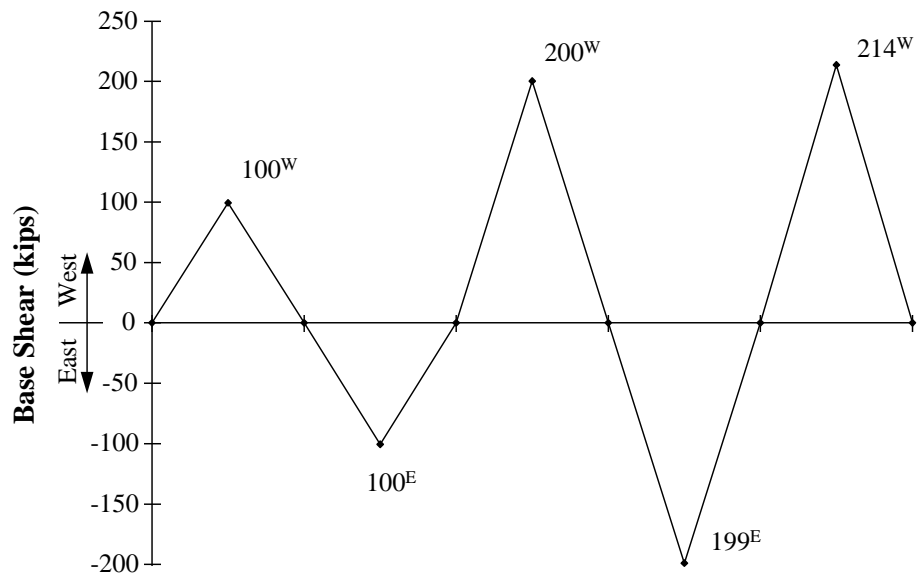


Figure 4.8: Door Test: Loading History

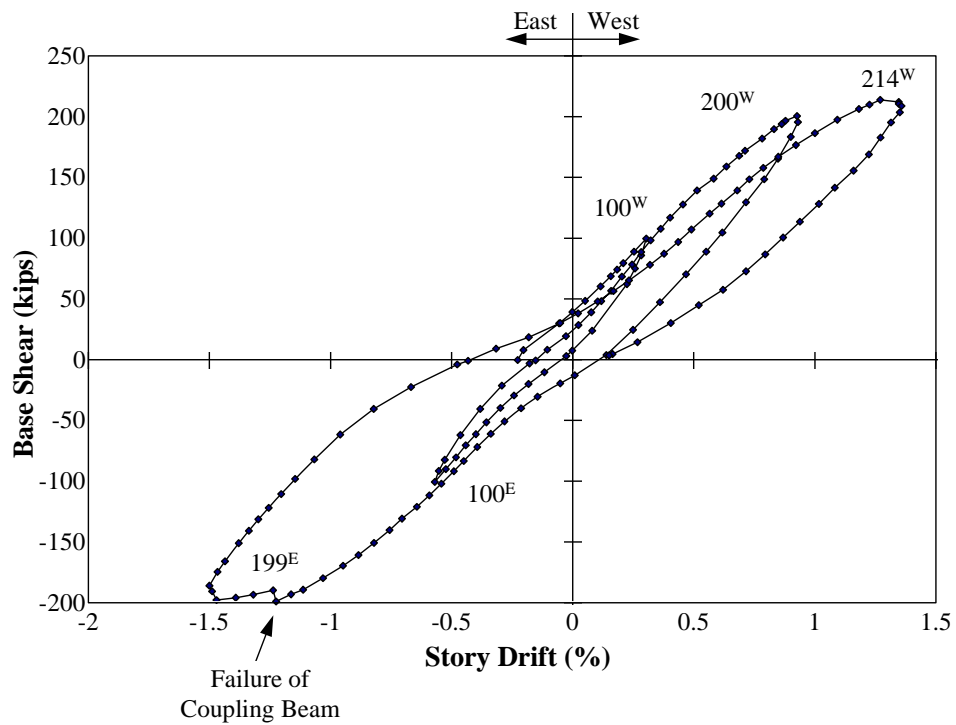


Figure 4.9: Door Test: Load vs. Drift Response

east cycle (to be described in the next section). At a load just over 200 kips, the shear crack which had begun to form in the beam over the door opening during the previous cycle grew and opened rapidly. The crack propagated into the third floor slab until loading was stopped. Failure of the coupling beam in this manner signified that the peak capacity of the wall system had been reached. The failed coupling beam is shown in Figure 4.10. It can be seen in this photo that the two components of the coupling beam, the existing frame beam and the horizontal grout strip, failed separately. When the coupling beam failed, the bars in the closure strip immediately to the right of the door yielded. The yielded bars buckled during subsequent unloading of the structure because the steel in the strip had no confining reinforcement. The buckled bars are shown in Figure 4.11. A base crack (shown in Figure 4.12) was observed to open during the higher load cycles at the base of the wall section to the right of the door. This portion of the wall section rotated about the toe of the wall.



**Figure 4.10: Failed Coupling Beam During West
Direction Loading**



Figure 4.11: Buckled Reinforcement in Closure Strip

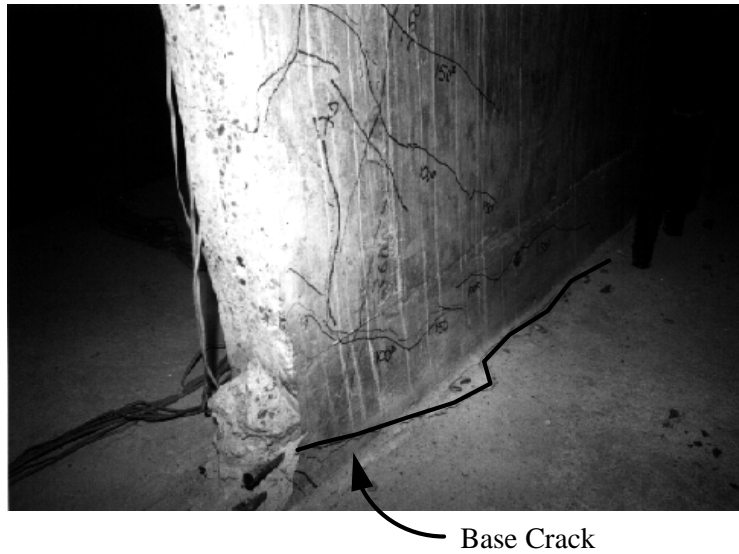


Figure 4.12: Base Crack at Doorway

4.3.2.2 East Direction

Behavior in the east direction closely mirrored that of the west direction. The first cycle to 100 kips produced little new cracking. During the second cycle, the stiffness began to decrease at approximately 150 kips base shear. In the wall to the left of the door, extensive existing cracks precluded formation of many new cracks, although some existing cracks extended and a few new cracks did appear at higher loads.

Between 190 kips and 200 kips, the coupling beam over the door failed in shear. The failed coupling beam is shown in Figure 4.13. Significant uplift occurred at the base of the wall to the left of the opening, and the vertical grout strip reinforcement yielded. Distress is apparent in this picture in the grout strip area around the pipe. On the other side of the door, the compression zone in the right wall section began to crush simultaneously. As for the west direction, the yielded bars buckled upon unloading because the steel in the strip had no confining reinforcement.



Figure 4.13: Failed Coupling Beam During East Direction Loading

CHAPTER 4	58
4.1 INTRODUCTION	58
4.2 WINDOW TEST.....	58
4.2.1 Preliminary Observations on Panel Removal.....	58
4.2.2 Structural Behavior.....	59
4.2.2.1 West Direction.....	60
4.2.2.2 East Direction	62
4.3 DOOR TEST.....	64
4.3.1 Preliminary Observations on Panel Removal.....	64
4.3.2 Structural Behavior.....	66
4.3.2.1 West Direction.....	66
4.3.2.2 East Direction	70
FIGURE 4. 1: CRACKS IN WINDOW PANEL PRIOR TO REMOVAL	59
FIGURE 4. 2: WINDOW TEST: LOADING HISTORY	61
FIGURE 4. 3: WINDOW TEST: LOAD VS-DRIFT RESPONSE	61
FIGURE 4. 4: DAMAGE DURING WINDOW TEST.....	63
FIGURE 4. 5: CRUSHING AT TOE OF WALL	63
FIGURE 4. 6: CRACKING AT FAILURE OF WINDOW CONFIGURATION	64
FIGURE 4. 7: DOOR CONFIGURATION.....	65
FIGURE 4. 8: LOAD DOOR TEST: LOADING HISTORY	67
FIGURE 4. 9: DOOR TEST: LOAD VS. DRIFT RESPONSE.....	67
FIGURE 4. 10: FAILED COUPLING BEAM DURING WEST DIRECTION LOADING	68
FIGURE 4. 11: BUCKLED REINFORCEMENT IN CLOSURE STRIP.....	69
FIGURE 4. 12: BASECRACK AT DOORWAY.....	69
FIGURE 4. 13: FAILED COUPLING BEAM DURING EAST DIRECTION LOADING	70

Error! No table of figures entries found.

CHAPTER 5

ANALYSIS

5.1 Introduction

In this chapter, experimental strength and stiffness data are compared with calculated results using conventional models of the test specimen. The comparisons demonstrate the applicability of different procedures for predicting infill wall behavior. The differences in behavior of the infill wall with and without openings are quantified. Finally, failure modes are examined to identify weaknesses created or exposed by the presence of openings in the structural system, and suggestions are offered for improving the system's performance in light of these observations.

5.2 Strength

5.2.1 Strength With and Without Openings

The base shear capacity of the 6 in. thick full infill wall without post-tensioning as tested by Frosch^[6] was 491 kips. The peak shear reached during the window test was 451 kips, or approximately 92% of the strength of the full infill. A maximum applied shear of 322 kips was applied to the 4 in. wall during the final shear test by Frosch, but was not sufficient to produce failure of the wall, so it is possible that the capacity of the 4 in. full infill is significantly higher than 322 kips. Based on the measured relationship of the 6 in. wall capacity to its nominal strength using ACI 318-95^[3], the estimated capacity of the 4 in. wall is between 360 and 420 kips. The applied base shears at failure of the 4 in. infill with the

door opening were 199 kips for the east and 214 kips for the west loading directions. These values are summarized in Table 5.1. Using these values, the strength of the 4 in. infill with door was between 47% and 69% of the strength of the 4 in. full infill. It is apparent that the removal of two vertically aligned panels to create a door opening had a much larger impact on the strength of the infill system (reduction of 40-50%) than the removal of a single panel to create a window opening (reduction of about 10%).

Table 5.1: Infill Strength with Openings

	Wall Strength (kips)	
	Full Infill	With Opening
6" Wall	491	451
4" Wall	360 - 420*	199-214

* Estimated strength based on ratio of 6" full infill shear strength to ACI strength.

5.2.2 Strength Prediction of Infill with Window

In Reference 6, Frosch recommends a capacity design approach for calculating the shear strength of the infill system. In this approach, the steel pipe shear lugs are designed as the weak links in the wall. Therefore, the design strength of the wall can be taken as the sum of the shear strengths of the pipes. Based on the nominal material strength of the three pipes at the base of the infill wall, the nominal capacity of the full infill system is 142 kips using Frosch's approach. Based on actual yield and ultimate pipe material strengths recorded in Section 2.6, the capacity of the wall is 217 kips and 290 kips, respectively. Recall that the tested strength of the full infill was 491 kips, so this method gives a very conservative design value for the wall's shear strength.

The capacity design approach can be used in the case of an infill with a window opening, with some caution. The opening may reduce the effectiveness of the group of shear lugs by redistributing the shear to less efficient paths. In the case of force application in the east direction, the middle shear lug at the top of the first story has effectively no material to resist its capacity, other than the concrete above the window. This force can only be transferred to the eastern-most lug, as shown in Figure 5.1. At this point the force must travel through a relatively steep (inefficient) compression strut to the toe of the wall. Unless the individual panels are each designed to exceed the capacity of two shear lugs, the design assumption may be unconservative. In the specimen, however, the tested strength of 451 kips still exceeded the highest calculated shear strength of the lugs, indicating that base shear is transferred through other mechanisms in addition to the shear lugs.

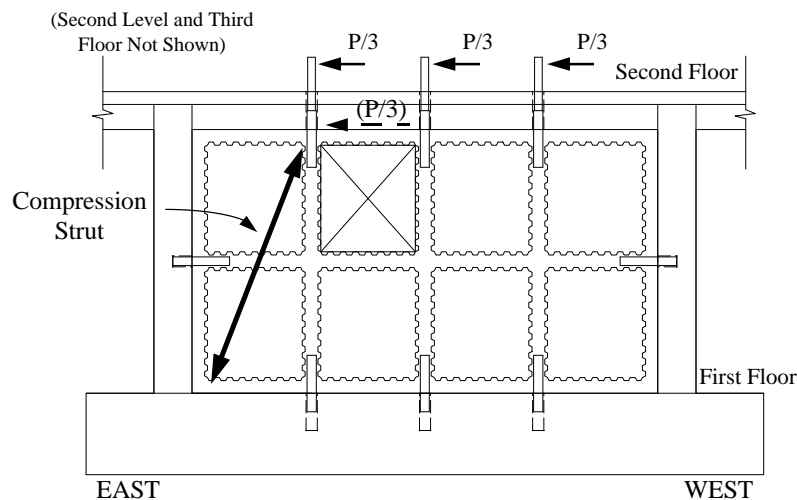


Figure 5.1: Force Flow Around Window

A convenient and familiar method for calculating the shear strength of a wall is given in the ACI Code. Although this method was developed for

monolithically constructed (cast-in-place) walls, the behavior of the specimen throughout testing indicated that the components of the precast infill system behave as a monolithic structure. Based on the ACI approach in Section 21.6, the calculated nominal strength of the wall with a window opening is 376 kips. The vertical steel in the outermost strips was not included in this calculation because it was not anchored at the top. Thus, the ACI method produces a better, but still conservative estimate of the shear wall's strength.

The desired failure mode for the infill wall system is the development of a flexural hinge at the base of the wall. Because this mode is more ductile than a shear failure mode, Frosch recommended that the wall be designed with sufficient shear capacity to develop its flexural capacity. Therefore, a conservative estimate of the shear strength is needed, along with an accurate estimate of the flexural strength. Base shears corresponding to the flexural capacity of the wall in either direction can be calculated using a rectangular stress block approach. The following assumptions were made:

- The yield strength of the post-tensioning bars is 90% of their nominal strength.
- The column bar splices fail before the post-tensioning bars yield, and therefore do not contribute to ultimate flexural strength. Splice failure occurred during the window test. It should be pointed out that if the splices do not fail before the post-tensioning bars yield, the wall shear strength should be designed to develop these bars as well. In the case of the test specimen, the calculated flexural capacity in both directions exceeded the calculated shear strength from each estimate.
- The window does not affect flexural capacity. In other words, the wall segments above and below the window are strong and stiff

enough to fully couple the system. The behavior of the specimen during testing supports this assumption.

Using these assumptions, the calculated flexural capacity of the wall corresponds to 425 kips of base shear in the west direction and 525 kips of base shear in the east direction. Because these numbers exceed the shear strength estimates, one would expect the wall to fail in shear (as was observed) rather than flexure.

Table 5.2: Summary of Calculated Strengths vs. Tested Strength for Infill with Window

Method	Base Shear (kips) @ Ultimate
Pipe - Nominal Yield	142
Pipe - Actual Yield	217
Pipe - Ultimate	290
ACI Shear	376
Flexure (East)	525
Test	451

5.2.3 Strength Prediction of Infill with Door

The effectiveness of all the shear lugs in the door configuration is even more questionable than that in the window configuration. In either loading direction, one shear lug at the base of the wall adjacent to the door cannot develop its capacity. Even if the shear lug had sufficient bearing embedment, it would not be fully effective because it is not along an efficient load path or compression strut (see Figure 5.2). For this reason, it seems appropriate to count only two

shear lugs for the purpose of calculating the shear strength of the infill with door using Frosch's method.

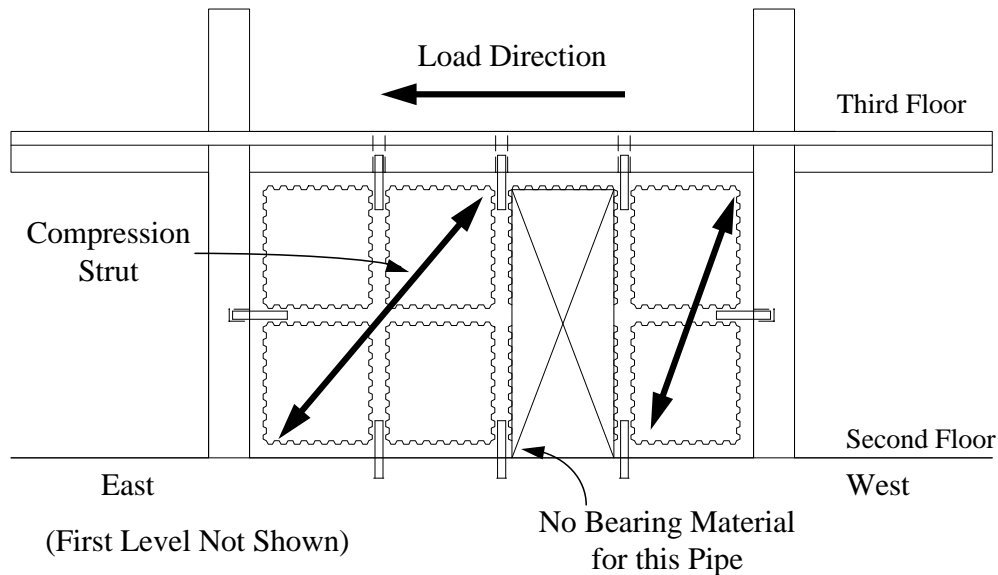


Figure 5.2: Compression Struts During Window Test

Based on values tabulated in Section 2.6, the nominal capacity of the two lugs is 62 kips, while their capacities at actual yield and ultimate material strengths are 72 kips and 99 kips, respectively. As was the case in the window and full infill tests, the actual strength of the wall with the door opening was much greater than that of the lugs alone, indicating that some other shear mechanisms are also at work at the interface.

Based on ACI shear equations in Sections 11.4, 11.5, and 21.6, the sum of the shear strengths of the columns and 4 in. wall segments is 243 kips. The shear strength of the columns is included because the column splices above the second level did not fail. Judging from the relative lack of shear distress witnessed in the

specimen during the door test, it seems likely that the wall could have reached at least 243 kips had a flexural-type failure not occurred first.

Accurately calculating the flexural capacity of the infill with door opening is more complicated than calculating its shear capacity. A range for the flexural capacity can be determined based on two different assumptions about the strength of the coupling beam over the door. A lower bound on the strength can be found by assuming that the coupling beam is very weak, resulting in two uncoupled wall segments. If one assumes that the coupling beam is very stiff and strong, the two wall segments will behave as a fully coupled system, giving an upper bound on the strength. Figure 5.3 depicts the flexural behavior of the infill with door opening assuming uncoupled and fully coupled behavior. In uncoupled behavior (Figure 5.3a), one wall segment has vertical steel in the closure strip(s) along the wall for tensile reinforcing, while the other segment can be assumed to use the post-tensioning bars as tensile steel. In fully coupled behavior (Figure 5.3b) both wall segments act together, and flexural capacity is calculated as for a full infill wall. The column on one end provides the compression block, while the post-tensioning bars at the other end are the primary tensile reinforcement.

The actual strength of the infill with door opening should fall somewhere between the values obtained from these two approaches. Base shears corresponding to flexural failure in uncoupled and fully coupled modes were calculated for the specimen using test data for the stresses (rather than nominal capacity stresses) in the post-tensioning rods at failure. It was assumed that the vertical strip reinforcement had reached its actual (tested) yield stress for purposes

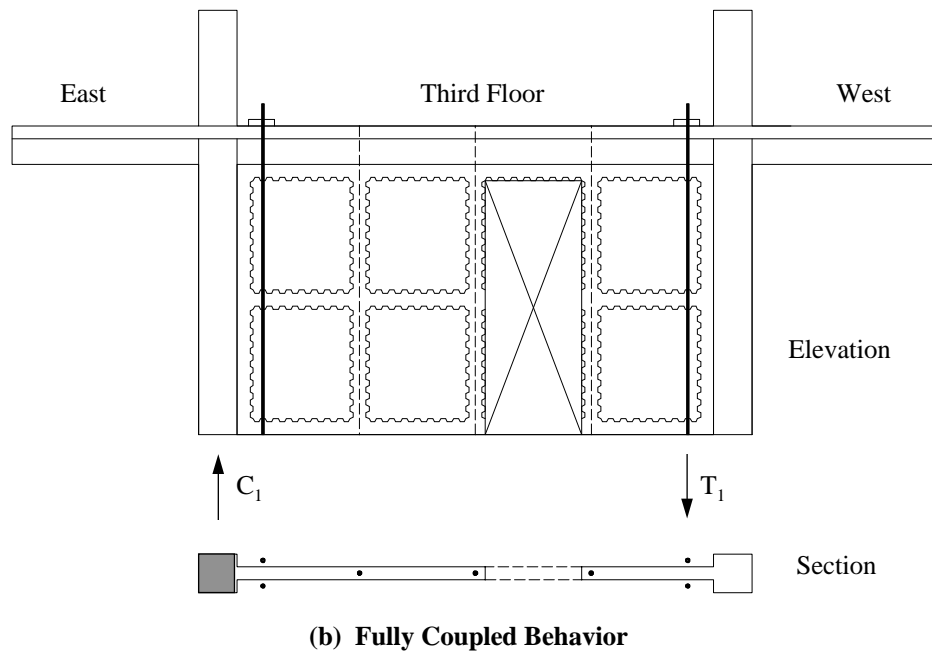
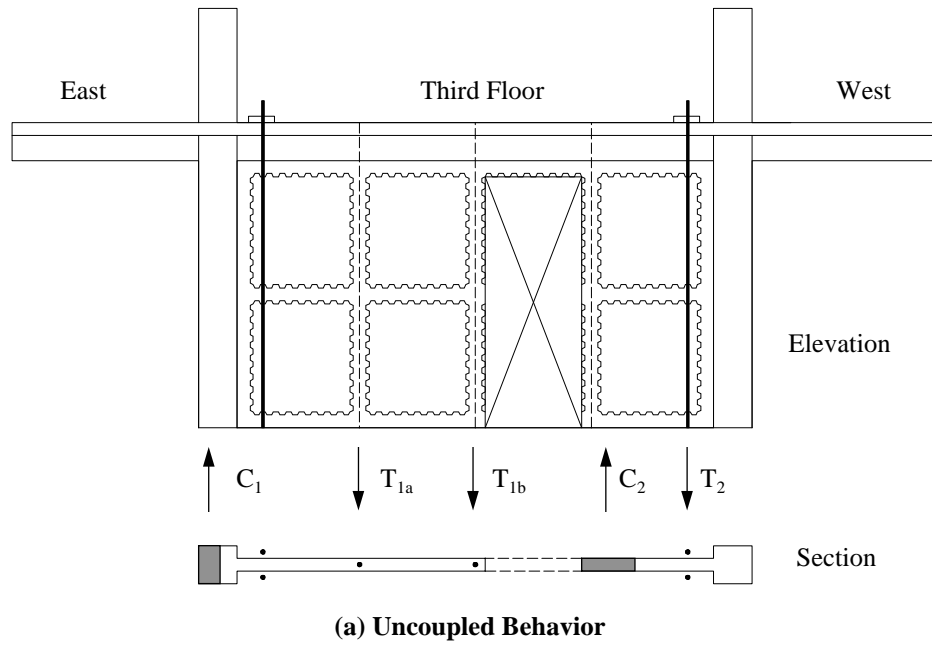


Figure 5.3: Uncoupled and Fully Coupled Behavior

of calculating uncoupled strength. The results of these calculations for both directions are shown in Table 5.3, along with actual failure loads.

Table 5.3: Flexural Strength of Infill with Door

Direction	Failure Load (kips)	
	West	East
Uncoupled	160	98.5
Fully Coupled	338	310
Test	214	199

As expected, the actual failure load is between the two calculated case values for each direction, and is somewhat closer to the uncoupled case than the fully coupled case. From the appearance of the walls after testing, it was expected that the system behaved more like the uncoupled case.

The beam over the door was not designed or detailed as a “coupling beam”, so it should not be expected to effectively couple the walls. Figure 5.4 shows a detail of the coupling beam region in the test specimen. Notice that the only top steel available at the negative beam moment sections is the welded wire fabric in the slab. In addition, only two of the three bottom bars extend continuously through the beam; the middle bar is interrupted by the core holes for the steel pipes. Finally, the stirrups stop at a distance less than d from the face of the opening. The reinforcing in the horizontal grout strip may help marginally, but there is no reason or evidence to expect it to act monolithically with the beam from the existing frame. FEMA^[4, 5] recommends that coupling beams be detailed with diagonal bars anchored in the wall segments and confined by special transverse reinforcement, neither of which are included in the existing frame coupling beam. In spite of these shortcomings, the presence of the weak coupling

beam allowed the wall to perform significantly better than an uncoupled wall would be expected to perform.

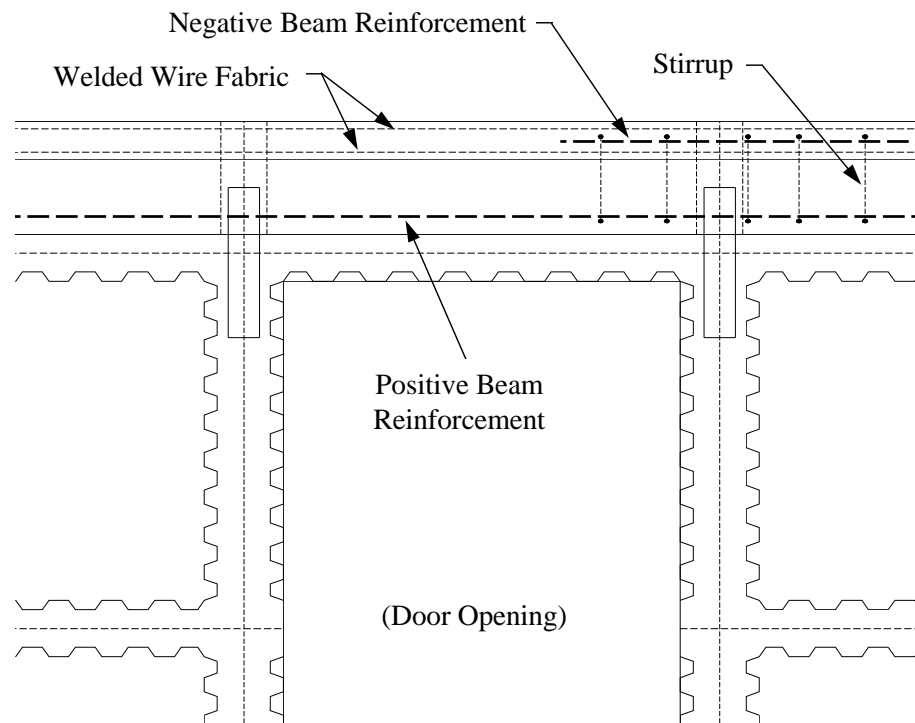


Figure 5.4: Coupling Beam Region

5.3 Stiffness

5.3.1 Introduction

Calculating the elastic stiffness of an infill wall is useful in seismic design for estimating drift ratios, which are indicative of the amount of structural and non-structural damage a building might suffer during an earthquake. A wall with openings is certainly less stiff than a wall without openings, but by how much?

Based on shear stiffness alone, it might be expected that the stiffness would vary directly with either cross-sectional area, or perhaps surface area of the wall. Using a cross-sectional area approach, the stiffness of the infill with either a door or a single-panel window would be about 3/4 of the stiffness of a four-panel wide full infill. Looking at the surface area of a two- by four- panel wall, the stiffness of a wall with one panel missing (window) might be 7/8 of the full infill stiffness, while a door configuration would have 6/8 of the full infill stiffness.

5.3.2 Methodology

The experimental stiffness of the wall in each of the configurations is compared with the experimental stiffness of the corresponding full infill in the test immediately preceding it. Thus, the results of the window test are compared with the last cycle of the full infill shear tests, and the door test is compared with the window test. This method minimizes the change in stiffness between tests due to damage occurring during tests.

The secant stiffnesses were compared at approximately 75% of the lowest peak load reached in the ultimate cycles of the two tests. Thus, the window was compared at 75% of 300 kips base shear, or 225 kips, and the door stiffness was compared at 75% of 199 kips base shear, or 150 kips. This method was chosen to eliminate the effects of damage that occur at higher load levels. Figure 5.5 illustrates this method for the window test.

Deflection values for comparing window stiffness were measured at the second level to exclude deflections of the 4 in. thick infill from consideration. As a result, the 6 in. thick infill with the window is compared directly with the 6 in. thick full infill. Obtaining deflections for stiffness calculation purposes for the door test is more difficult because of a difference in loading methods. Recall that

the door test was performed with the rams locked off at the second level, and load was applied only at the third floor. In effect, the wall being tested was only one story high because the second floor was restrained from translating. The window test was performed over the full specimen height with load being applied at both the second and third floors. To calculate the stiffness of only the 4 in. full infill at the second level, the interstory drift was obtained by subtracting the measured deflection at the second level from the deflection at the third level. The load used was only that which contributed to shear in the 4 in. wall: the load applied at the third level.

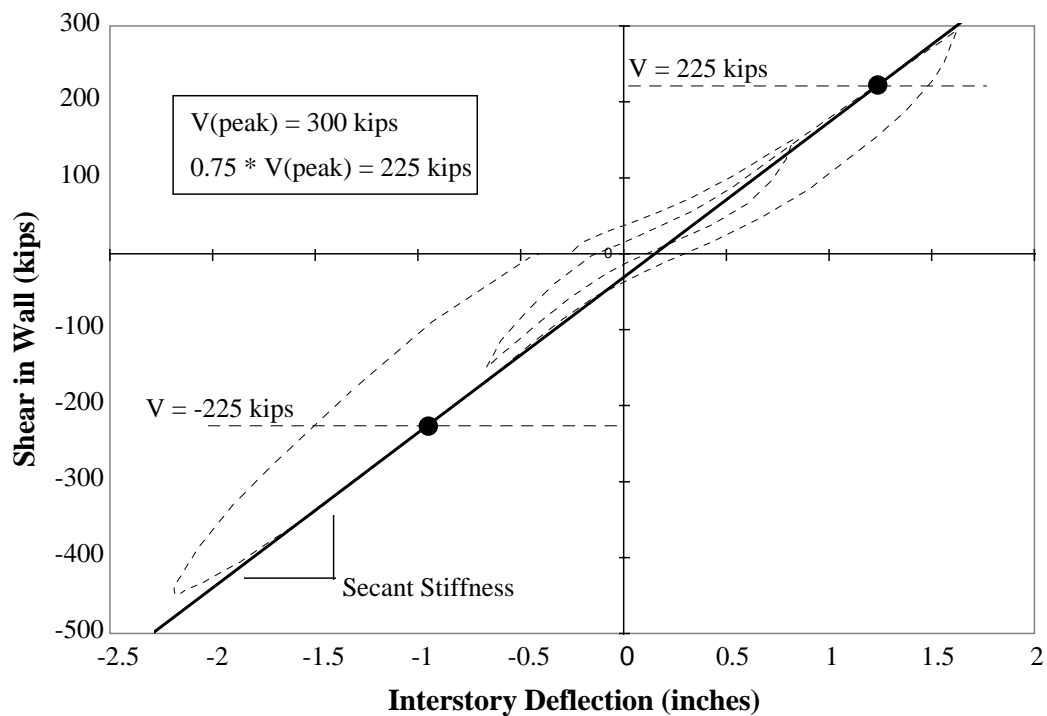


Figure 5.5: Secant Stiffness Determination (Window Test Shown)

Further complicating the deflection determination for the 4 in. infill stiffness is the influence of rigid body rotation of the wall. During the window test, an uplift of about 3/4 in. was observed at the base of the wall. The failed bar

splices in the columns allowed the wall to rotate as a rigid body through some angle, θ (see Figure 5.6). This rotation alone produces a measured deflection of $h\theta$ at the second level and $2h\theta$ at the third level, where h is the height of one story (8 feet). When the difference is taken between the deflections at the second and third floors, a net deflection of $h\theta$ remains which has nothing to do with the shear stiffness of the 4 in. wall. This rigid body rotation effect must be subtracted to accurately compare the stiffness of the full infill with that of the infill with door. Rigid body rotation effects are minimal in the door test because the column splices did not fail, and no significant uplift of the wall was noted until the wall reached its ultimate capacity. Three methods used in estimating rigid body rotation effects during the window tests are outlined in the following section.

A simple analytical model of the specimen was also created using the SAP90^[8] program. Cracked section properties were used for the frame with each panel being represented by a finite element. Each finite element corner was attached to the frame and/or adjacent finite elements. Because of the flexural crack at the base of the wall and the failed column bar splices, the base of the wall was modeled as unrestrained, except at the toe of the wall, for the 6 in. wall comparison. For the 4 in. wall comparison, the second floor was restrained from translating, and the base of the wall (now considered at the second floor) was left attached to the frame because the column splices were intact at that level.

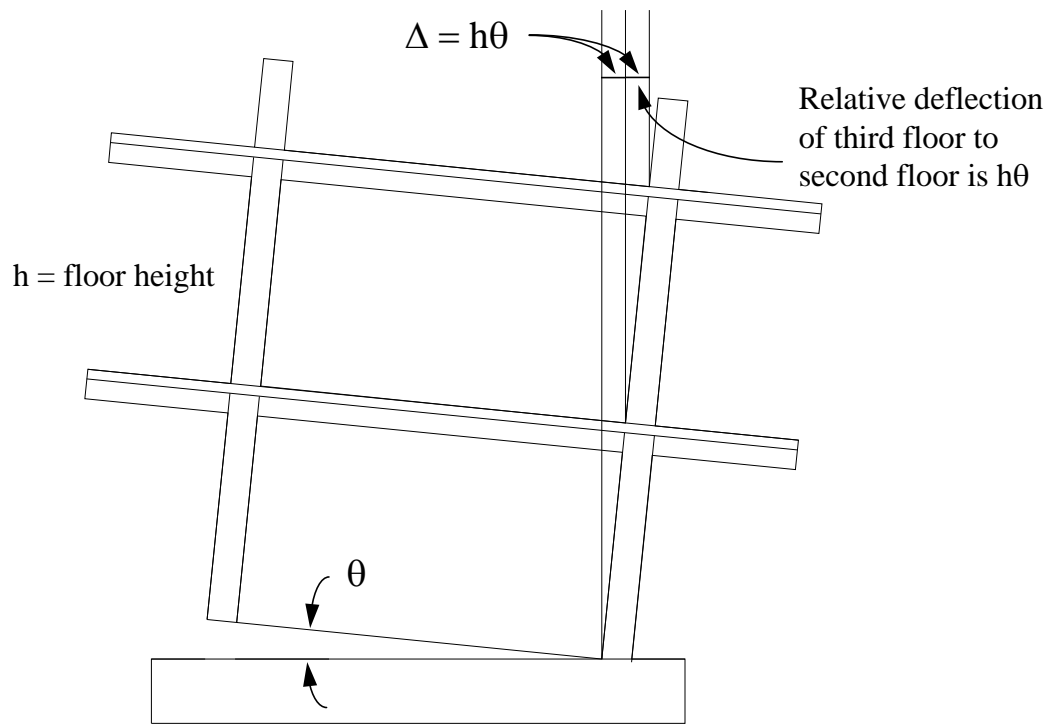


Figure 5.6: Rigid Body Rotation Effects

5.3.3 Stiffness Comparisons

5.3.3.1 Window Test

The stiffness of the wall during the window test in the east and west directions can be compared to the full infill stiffness during the final shear test, in which load was applied in the east direction only. Comparable full infill data are not available for the west direction because load was not applied in that direction without precompression supplied by the external post-tensioning bars. However, the stiffness of the full infill should be approximately equal in both directions. Table 5.4 summarizes the results of the stiffness comparison for the window test.

Table 5.4: Stiffness Comparison: Window vs. Full Infill

Load Case	% of Full Infill Stiffness
East	72
West	55
Avg.	64

From this data, it appears that the stiffness of the wall with a single panel window is about two-thirds that of a full infill. The SAP90 model predicted that the window configuration would be minimally less stiff (by about 2%) than the full infill, and does not appear to accurately evaluate the relative stiffness of the wall conditions in this case.

5.3.3.2 Door Test

For the door test, the second half-cycle in either direction was chosen to compare with the final east and west cycles from the window test. Recall the coupling beam failed at the end of the second cycle during load application in the east direction. Afterwards, the wall was taken to failure in the west direction. The final west half-cycle (after coupling beam failure) exhibited approximately 80% of the stiffness of the previous west half-cycle to 200 kips (before coupling beam failure). Thus, it was chosen to use pre-coupling beam failure data for comparison purposes to eliminate the effects of coupling beam failure on wall stiffness.

For both the door and the window tests, there was negligible difference between the 4 in. wall results in either loading direction. Without making any adjustments to correct the window test data for rigid body rotation effects, the

stiffness of the infill with door appears to be approximately 80% of the full infill stiffness. Note that these results indicate that the wall is stiffer with the door (two panels missing) than a window (one panel missing), which is not logical. However, rigid body rotation effects must be subtracted in order to obtain an accurate comparison.

Three methods were used to estimate the rigid body rotation of the structure. All three involve some measurement of vertical displacements to get an angle of rotation, with the tangent of a small angle being approximately equal to that angle. Thus, as described in Section 5.3.2, the displacement of the third floor relative to the second floor is the floor height times that angle ($h\theta$). All three methods are illustrated in Figure 5.7.

The first method is based on the observation that the gap between the base of the wall and the top of the footing was measured to be $3/4$ in. at the ultimate load (451 kips base shear) during the window test. Assuming the gap varies linearly with load, this results in an estimated gap width of ($3/4$ in.) times (225 kips/ 451 kips) at the secant stiffness point. The angle θ is obtained by dividing the proportional gap by the length of the wall, 12 ft. - 4 in.

The second and third methods are closely related, making use of the data obtained from vertically oriented linear pots located at each floor level at either end of the structure. In the second method, the angle is obtained by adding the upward deflection at one end to the downward deflection at the other end and dividing by the length of the floor (24 feet). For the third method, only the upward deflection is used, and that value is divided by the distance from one end of the structure to the inside face of the opposite column, assuming that this is the center of rotation of the wall.

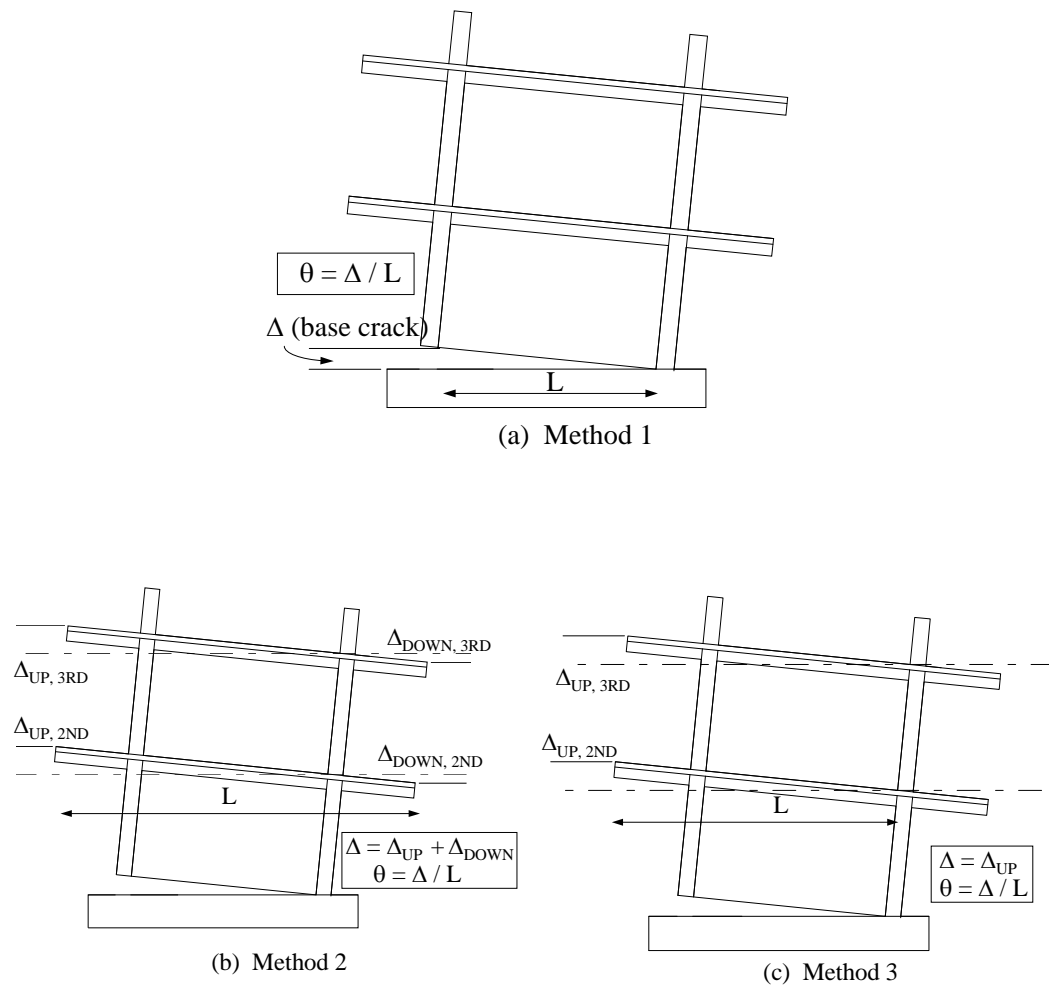


Figure 5.7: Three Methods of Determining Rigid Body Rotation Effects

The stiffness corrected using measured rigid body rotation from the three approaches is summarized in Table 5.5.

Table 5.5: Stiffness Comparison: Door vs. Full Infill

Method	Load Case	% of Full Infill Stiffness
1	E	37.4
	W	36.7
2	E	24.7
	W	~1
3	E	32.4
	W	6.0

All three methods produce fairly consistent results for the east direction, but results vary significantly for the west direction. The small stiffness ratios shown in the west direction for methods 2 and 3 are likely to have resulted from vertical displacements due to sources other than rigid body rotation of the wall. In the west direction, the rams push on the structure, causing uplift at the end of the structure where the rams are attached. The uplift and corresponding inclination of the rams generates a vertical force component, which creates flexure in the floor slab as it cantilevers out from the centerline of the structure. Because vertical deflections are measured away from the centerline, the linear pots measure deflection due to flexure in the slab as well as rigid body rotation, which is additive. The end result is a larger estimated angle of rotation, and smaller apparent stiffness for the west load cases for methods 2 and 3.

The SAP90 computer model predicts a stiffness ratio of 42% for the door test. This is slightly higher than the experimental data which suggest that the stiffness of the infill with door is between 1/4 and 1/3 that of a full infill. The SAP90 model appears to better predict relative stiffnesses for cases in which the column splices are intact than for cases in which they have failed.

5.4 Design and Construction Needs of Infills with Openings

Based on the observed behavior of the specimen during testing, some special needs can be identified to improve the development of the strength of the infill wall with openings.

First, a lesson from the window test. For an infill with a window (or a door), it is important to take into account the reduced shear strength of the wall during design. To ensure flexural failure of the wall rather than a shear failure, it may be necessary to apply precompression to the wall via the post-tensioning bars. Alternatively, the flexural capacity may be reduced by using a smaller area of post-tensioning steel at either end.

More serious design modifications may be required to correct problems observed in the door test configuration. Two main areas of concern stand out: the coupling beam and the vertical strips along either side of the door.

Because of its size and reinforcement, the coupling beam is neither strong nor stiff. It is not designed and detailed to serve as a “coupling beam”, and its failure should be expected. The coupling beam is likely to fail in a brittle manner due to the termination of top reinforcement and lack of stirrups along its length. Help for the coupling beam’s strength could be provided by a wall (if one exists) directly above the beam. Also, beam jacketing could be employed to increase the strength or ductility of the coupling beam. This could be done at the same time the infill wall is installed. The stronger and stiffer the coupling beam is, the stiffer the infill wall system will be, and the higher the peak load it is likely to resist. If possible, the coupling beam should be designed to allow the wall to develop its fully coupled flexural strength.

The strength and performance of the wall with a door opening could also be improved by the creation of small boundary elements along each side of the door. This could also be done at the same time the infill wall is installed. These

boundary elements would provide more room for additional vertical reinforcement, which would increase the flexural capacity of a wall which is expected to behave as a partially coupled system. Additionally, confinement steel could be added to prevent the vertical bars from buckling after they yield. The large amount of debris observed in the doorway due to reinforcement buckling during testing could create an exit hazard during a seismic event.

CHAPTER 5.....	71
5.1 INTRODUCTION	71
5.2 STRENGTH	71
5.2.1 <i>Strength With and Without Openings</i>	71
5.2.2 <i>Strength Prediction of Infill with Window</i>	72
5.2.3 <i>Strength Prediction of Infill with Door</i>	75
5.3 STIFFNESS.....	80
5.3.1 <i>Introduction</i>	80
5.3.2 <i>Methodology</i>	81
5.3.3 <i>Stiffness Comparisons</i>	84
5.3.3.1 <i>Window Test</i>	84
5.3.3.2 <i>Door Test</i>	85
5.4 DESIGN AND CONSTRUCTION NEEDS OF INFILLS WITH OPENINGS	89
FIGURE 5. 1: FORCE FLOW AROUND WINDOW.....	73
FIGURE 5. 2: COMPRESSION STRUTS DURING WINDOW TEST	76
FIGURE 5. 3: UNCOUPLED AND FULLY COUPLED BEHAVIOR	78
FIGURE 5. 4: COUPLING BEAM REGION.....	80
FIGURE 5. 5: SECANT STIFFNESS DETERMINATION (WINDOW TEST SHOWN)	82
FIGURE 5. 6: RIGID BODY ROTATION EFFECTS	84
FIGURE 5. 7: THREE METHODS OF DETERMINING RIGID BODY ROTATION EFFECTS.....	87
TABLE 5. 1: INFILL STRENGTH WITH OPENINGS	72
TABLE 5. 2: SUMMARY OF CALCULATED STRENGTHS VS. TESTED STRENGTH FOR INFILL WITH WINDOW	75
TABLE 5. 3: FLEXURAL STRENGTH OF INFILL WITH DOOR	79
TABLE 5. 4: STIFFNESS COMPARISON: WINDOW VS. FULL INFILL	85

TABLE 5. 5: STIFFNESS COMPARISON: DOOR VS. FULL INFILL 87

CHAPTER 6

SUMMARY AND CONCLUSIONS

6.1 Summary

Many existing structures are in need of seismic rehabilitation to avoid undergoing catastrophic collapse during a severe seismic event. One obstacle standing in the way of a more rapid, broad-scope rehabilitation movement for nonductile structures is the cost of strengthening them. A potentially economical method of strengthening has been developed which uses precast concrete panels to create an infill wall in a concrete frame building. A large-scale model using this method has been tested with positive results at the University of Texas' Phil M. Ferguson Structural Engineering Laboratory.

Architectural requirements may necessitate windows or doors in bays where infill walls are located. To examine the effects of such openings on the precast panel infill system, further tests were conducted on the same large-scale model with a window and a door opening in place.

Crushing at the toe of the wall, followed by a shear failure through the wall panels marked the development of ultimate strength during the window test. Yielding of vertical strip reinforcement and failure of the coupling beam above the door defined the failure of the infill with door. During these tests, as in previous tests, the precast panels and cast-in-place closure strips acted monolithically to bypass the weaknesses of the existing frame.

6.2 Conclusions and Recommendations

The design of a precast panel infill wall with openings can be an effective means for strengthening nonductile reinforced concrete structures. The openings affect the behavior of the wall, and may require design modifications to produce an effective system. The following conclusions can be drawn from the tests:

- 1.) *Openings reduce the shear strength of the wall.* The method of calculating shear strength recommended by Frosch^[6] produces conservative results for a capacity-type design. Consideration during design should be given to the effectiveness of shear lugs located near openings, which can create force flow problems. The ACI 318-95^[3] equations for shear strength produce conservative design shear strengths which appear to give a more accurate estimate of the actual strength of the infill.
- 2.) *Openings can reduce the flexural strength of the infill.* Particularly in the case of the infill with door, the wall system is likely to perform at some flexural strength level below that of a fully-coupled system, but possibly above that of an uncoupled system.
- 3.) *Openings reduced the stiffness of the infill.* The wall with a single-panel window opening was approximately 2/3 as stiff as a full infill. The infill with a door opening was about 1/4 to 1/3 as stiff as the full infill.
- 4.) *Some design modifications may be required to rectify the exposure of new “weak links” in the system by the openings.* Of particular concern are the coupling beam over the door (which can be modified by jacketing) and the vertical strip steel on each side of the door (which can be improved by creating boundary elements).

The precast infill system as constructed in the test specimen appears capable of accommodating openings and developing significant strength, but design modifications could serve to further increase the strength and integrity of the system. Whether or not design improvements to the existing frame are implemented, the goal in design should be to have sufficient shear strength to develop the flexural capacity of the wall. Realizing that for short walls this may be impractical, a shear capacity design is acceptable if the lower ductility of this failure mode is taken into account during design.

BIBLIOGRAPHY

1. ACI Committee 318, "Building Code Requirements for Reinforced Concrete," ACI 318-56, American Concrete Institute, Detroit, 1956.
2. ACI Committee 318, "Building Code Requirements for Reinforced Concrete," ACI 318-63, American Concrete Institute, Detroit, 1963.
3. ACI Committee 318, "Building Code Requirements for Reinforced Concrete," ACI 318-95, American Concrete Institute, Detroit, 1995.
4. FEMA-178, *NEHRP Handbook for the Seismic Evaluation of Existing Buildings*, Building Seismic Safety Council, Washington DC, 1992.
5. FEMA-222, *NEHRP Recommended Provisions for the Development of Seismic Regulations for New Buildings*, Building Seismic Safety Council, Washington DC, 1991.
6. Frosch, R. J., "Seismic Rehabilitation Using Precast Infill Walls," *Ph.D. Dissertation*, The University of Texas at Austin, May 1996, 234 pp.
7. Gaynor, P. J., "The Effect of Openings on the Cyclic Behavior of Shear Walls," *M.S. Thesis*, The University of Texas at Austin, May 1988, 245 pp.
8. Habibullah, A., & Wilson, E. L., *SAP90* [Computer program], Computers & Structures, Inc., Berkeley, CA, 1990.
9. Jimenez, L. R., "Strengthening RC Frames Using an Eccentric Wall," *M.S. Thesis*, The University of Texas at Austin, May 1989, 67 pp.
10. Shah, S. N., "Evaluation of Infill Wall Strengthening Schemes for Non-Ductile RC Buildings," *M.S. Thesis*, The University of Texas at Austin, May 1989, 68 pp.
11. UBC, *Uniform Building Code*, International Conference of Building Code Officials, Whittier, CA, 1955.

VITA

Michael Lee Brack was born in Wichita, Kansas on July 22, 1972, the son of Shirley Jean Brack and George Allen Brack. In 1990, Michael graduated Summa Cum Laude from Mac Arthur High School in San Antonio, Texas. Thereafter, he attended The University of Texas at Austin in the Plan II Liberal Arts Honors/Civil Engineering program. In December, 1994, he received two degrees Summa Cum Laude, a Bachelor of Science and a Bachelor of Arts, and was recognized as the Outstanding Scholar-Leader at the College of Engineering's graduation ceremony. The following January, Michael entered the Graduate School at the University of Texas at Austin in the Structural Engineering program. In January, 1996, he began his career at the Austin office of Datum Engineering, Incorporated.

Permanent Address: 6908 Gaur Dr.
Austin, Texas 78749

This thesis was typed by the author.

CHAPTER 6	91
6.1 SUMMARY	91
6.2 CONCLUSIONS AND RECOMMENDATIONS	92

BIBLIOGRAPHY

1. ACI Committee 318, "Building Code Requirements for Reinforced Concrete," ACI 318-56, American Concrete Institute, Detroit, 1956.
2. ACI Committee 318, "Building Code Requirements for Reinforced Concrete," ACI 318-63, American Concrete Institute, Detroit, 1963.
3. ACI Committee 318, "Building Code Requirements for Reinforced Concrete," ACI 318-95, American Concrete Institute, Detroit, 1995.
4. FEMA-178, *NEHRP Handbook for the Seismic Evaluation of Existing Buildings*, Building Seismic Safety Council, Washington DC, 1992.
5. FEMA-222, *NEHRP Recommended Provisions for the Development of Seismic Regulations for New Buildings*, Building Seismic Safety Council, Washington DC, 1991.
6. Frosch, R. J., "Seismic Rehabilitation Using Precast Infill Walls," *Ph.D. Dissertation*, The University of Texas at Austin, May 1996, 234 pp.
7. Gaynor, P. J., "The Effect of Openings on the Cyclic Behavior of Shear Walls," *M.S. Thesis*, The University of Texas at Austin, May 1988, 245 pp.
8. Habibullah, A., & Wilson, E. L., *SAP90* [Computer program], Computers & Structures, Inc., Berkeley, CA, 1990.
9. Jimenez, L. R., "Strengthening RC Frames Using an Eccentric Wall," *M.S. Thesis*, The University of Texas at Austin, May 1989, 67 pp.
10. Shah, S. N., "Evaluation of Infill Wall Strengthening Schemes for Non-Ductile RC Buildings," *M.S. Thesis*, The University of Texas at Austin, May 1989, 68 pp.
11. UBC, *Uniform Building Code*, International Conference of Building Code Officials, Whittier, CA, 1955.

VITA

Michael Lee Brack was born in Wichita, Kansas on July 22, 1972, the son of Shirley Jean Brack and George Allen Brack. In 1990, Michael graduated Summa Cum Laude from Mac Arthur High School in San Antonio, Texas. Thereafter, he attended The University of Texas at Austin in the Plan II Liberal Arts Honors/Civil Engineering program. In December, 1994, he received two degrees Summa Cum Laude, a Bachelor of Science and a Bachelor of Arts, and was recognized as the Outstanding Scholar-Leader at the College of Engineering's graduation ceremony. The following January, Michael entered the Graduate School at the University of Texas at Austin in the Structural Engineering program. In January, 1996, he began his career at the Austin office of Datum Engineering, Incorporated.

Permanent Address: 6908 Gaur Dr.
Austin, Texas 78749

This thesis was typed by the author.

CHAPTER 6 Error! Bookmark not defined.
6.1 SUMMARY **Error! Bookmark not defined.**
6.2 CONCLUSIONS AND RECOMMENDATIONS **Error! Bookmark not defined.**